Available online at www.sciencedirect.com
SCIENCE DIRECT®
Bioorganic & Medicinal Chemistry
ELSEVIER
Bioorganic & Medicinal Chemistry 13 (2005) 4383–4388

Synthesis of new phorbol derivatives having ethereal side chain and evaluation of their anti-HIV activity

Yuji Matsuya,[a] Zhong Yu,[b] Naoki Yamamoto,[b] Masao Mori,[c] Haruo Saito,[c] Makoto Takeuchi,[c] Mamiko Ito[c] and Hideo Nemoto[a,*]

[a]*Faculty of Pharmaceutical Sciences, Toyama Medical and Pharmaceutical University, 2630 Sugitani, Toyama 930-0914, Japan*
[b]*Department of Microbiology, Tokyo Medical and Dental University School of Medicine, 1-5-45 Yushima, Bunkyo-ku, Tokyo 113-8519, Japan*
[c]*Lead Chemical Co. Ltd, 77-3 Himata, Toyama 930-0912, Japan*

Received 5 April 2005; revised 21 April 2005; accepted 21 April 2005
Available online 23 May 2005

Abstract—Several new phorbol derivatives having ethereal substituents at the 12-position were synthesized and subjected to biological evaluation to find new candidates of an anti-HIV agent. Among them, 12-*O*-(methoxymethyl)phorbol 13-decanoate showed potent inhibitory activity against infection of HIV-1 in MT-4 cells (EC_{50}: 1.3 ng/mL) and relatively low cytotoxicity (CC_{50}: 8.3 μg/mL). This compound was also found to have sufficient stability in mouse plasma compared with the corresponding 12-acetate derivative, which was an equipotent HIV-1 inhibitor, but with an activity that decreased considerably after plasma treatment.

1. Introduction

According to the worldwide spread of acquired immunodeficiency syndrome (AIDS), development of an anti-HIV drug has been made widely for extermination of the causative agent. Many compounds originating from plants have been investigated to find a new potent inhibitor of the replication of HIV-1 or its essential enzymes.[1] Recently, phorbol esters isolated from the seed of *Croton tiglium* were reported to show anti-HIV-1 activity in vitro.[2] Phorbol esters have been reported to exhibit a wide variety of biological activities, including inflammation, cell proliferation, platelet activation, and many other biological responses.[3] Especially, tumor-promoting activity as well as the mechanisms of its causal PKC activation has been studied extensively.[4] Also, much research has revealed that these biological effects can be influenced by the nature (lipophilicity and hydrophilicity) and the structure (carbon-chain length, etc.) of the substituents on the C12- and/or C13-hydroxyl group(s) of the parent phorbol (Fig. 1).[5] Indeed, for example, it was disclosed that tuning of the C-12 ester moiety is an essential determinant of PKC agonist/antagonist activity.[6] With regard to anti-HIV-1 activity, TPA (12-*O*-tetradecanoylphorbol 13-acetate)[7] and prostratin (12-deoxyphorbol 13-acetate)[8] have been reported to have the HIV-1 inhibitory effect, the former of which acts with direct PKC activation and the latter without such a tumor-promoting action. Recently, a comprehensive study of the structure–activity relationship of phorbol esters has been performed on inhibition of an HIV-1-induced cytopathic effect. Among the many phorbol esters examined, 12-*O*-acetylphorbol 13-decanoate (**3**) was found to be the most effective inhibitor of HIV-1, obtained from culture supernatant of MOLT-4 cells, which were persistently infected with LAV-1.[9] Additionally, it did not influence

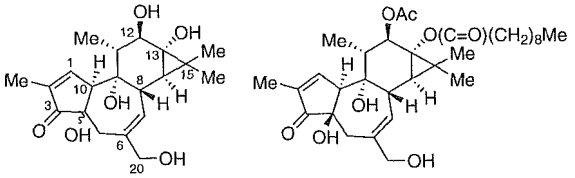

Figure 1. Parent phorbol and its known derivatives.

Keywords: Phorbol; Anti-HIV agents; Ethereal side chain; Safety index.
* Corresponding author. Tel.: +81 76 434 7530; fax: +81 76 434 5047; e-mail: nemotoh@ms.toyama-mpu.ac.jp

0968-0896/$ - see front matter © 2005 Elsevier Ltd. All rights reserved.
doi:10.1016/j.bmc.2005.04.056

the cell growth and viability of MT-4 cells at a concentration exhibiting anti-HIV-1 activity.[2,9]

In this study, we evaluated the anti-HIV-1 activity of compound **3** and its stability in a living body, and newly found that the activity was considerably decreased by pre-incubation with mouse plasma. Furthermore to search for much more stable and potent HIV-1 inhibitors under physiological conditions, we investigated the synthesis and the bioactivity of new 12-*O*-alkylated and α-oxyalkylated phorbol derivatives, as well as their in vivo stability and safety.

2. Results and discussion

2.1. Chemistry

We designed new phorbol derivatives possessing a decanoyloxy group on the 13-position and an ethereal linkage on the 12-hydroxyl group, in light of the previous finding about the suitable chain length of the acyl group at the 13-position[9] and the expected in vivo stability. Parent phorbol (**1**), which is available by the reported procedure[10] or from commercial sources, has five hydroxyl groups of different reactivity. The method for stepwise introduction of substituents onto each hydroxyl group has been well established for the preparation of various phorbol 12- and 13-diesters, the representative of which employ a trityl ether as a protection of the most reactive primary hydroxyl group at the 20-position.[11] This protecting group is removable by treatment with perchloric acid; however, because one of our synthetic goals is to introduce α-oxyalkyl groups to 12-oxygen, which are expected to be susceptible to hydrolysis under acidic conditions, we chose the TBS group for protection of the 20-hydroxyl group. Thus, the synthesis was performed according to Scheme 1.

The protection of the primary alcohol of parent phorbol (**1**) as a corresponding TBS ether (**4**) was carried out under the standard condition using TBS chloride and imidazole in DMF in 61% yield. Introduction of the decanoyl group to tertiary 13-OH was achieved by treatment with decanoyl chloride and triethylamine in CH_2Cl_2 with a high selectivity, probably due to the orientation of the 13-OH to less hindered space compared to the other hydroxyl groups, including the secondary 12-OH group. On the other hand, when using pyridine as a base, competitive 12-acylation was observed to afford the mixture of the product **5** and the 12-decanoyl isomer (ca. 2:1) concomitant with a small amount of 12,13-diacylated product. The structure assignment could be simply carried out based on the change of the chemical shifts of the 12-proton in their ^1H NMR spectra. The 13-decanoyl-derivative **5** was subsequently subjected to etherification at the 12-position; namely, methoxymethyl, (methoxy)ethoxymethyl, and benzyloxymethyl derivatives (**6a–c**, respectively) were synthesized by reaction with the corresponding chlorides in the presence of diisopropylethylamine, and additionally, 12-ethyl ether (**6d**) using ethyl triflate and 2,6-di-*tert*-butyl-4-methylpyridine. The compounds **6a–d** were allowed to react with TBAF in THF at room temperature to afford the deprotected products **7a–d** in high yields. Thus, our target phorbol derivatives having 12-ethereal side chains were satisfactorily synthesized in four steps from parent phorbol (**1**). In addition, 20-*O*-methyl-12-*O*-methoxymethylphorbol 13-decanoate (**8**) was also prepared from **7a** for the purpose of comparison of the bioactivity.

2.2. Biology

12-*O*-Acetylphorbol 13-decanoate (**3**), reported to be the most effective anti-HIV-1 phorbol derivative without PKC activation,[9] was examined for inhibitory activity against HIV-1 infection in MT-4 cells with and without pre-incubation with mouse plasma. The results are summarized in Table 1. As previously reported, the compound **3** potently inhibited the infection of HIV-1 in MT-4 cells (EC_{50}: 1.7 ng/mL), and its cytotoxicity in uninfected MT-4 cells was weak (CC_{50}: 3.3 μg/mL). On the other hand, the inhibitory activity of **3** against

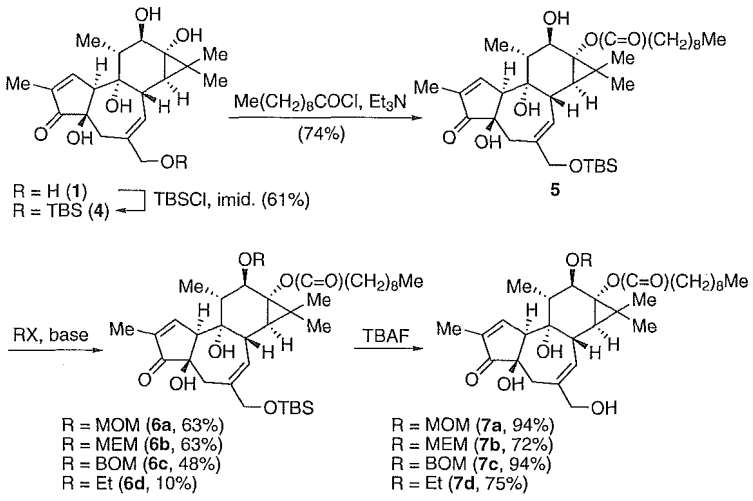

Scheme 1. Synthesis of 12-*O*-alkylphorbol 13-decanoate derivatives.

Table 1. Comparison of anti-HIV activity of 12-*O*-acetylphorbol 13-decanoate (**3**) in MT-4 cells with and without mouse plasma pretreatment

Entry	Plasma	Anti-HIV activity (EC_{50}, ng/mL)	Cytotoxicity (CC_{50}, μg/mL)	Safety index (CC_{50}/EC_{50})
1	–	1.7	3.3	1941
2	+	70.7	>10,000	>10,000

HIV-1 was obviously decreased after incubation with mouse plasma (EC_{50}: 70.7 ng/mL), suggesting a lack of in vivo efficacy as an anti-HIV agent.

We presumed that the undesirable aspect might be attributed to the inherent instability of **3** and consequential inactivation by a certain kind of enzyme (maybe pseudocholine esterase) under physiological circumstances. Assuming that the instability originates from susceptibility of the ester bond to hydrolytic degradation, new phorbol derivatives synthesized in this study, having 12-ethereal side chain rather than ester function, would be expected to show a proper stability and good in vivo efficacy. Thus, the modified compounds (**7a–d**, and **8**), as well as the basal compounds phorbol (**1**) and isophorbol (**2**), were evaluated for inhibition of infection of HIV-1 in MT-4 cells. Cytotoxicity in uninfected MT-4 cells was also determined, and the selectivity indexes were calculated based on the ratio of CC_{50} to EC_{50} values. These results are listed in Table 2.

The change of the acetyl group at the 12-position in **3** to the methoxymethyl group (**7a**) brought about the almost equipotent activity against HIV-1 to that of **3** (entries 3 and 4), and it was found that the activity was not reduced by pretreatment with plasma (Table 3). Furthermore, its CC_{50} value was ca. 2.5-fold as compared with that of **3**. However, extension of the 12-side chain to (methoxy)ethoxymethyl group (**7b**) led to slight decrease in inhibitory activity (entry 5). Introduction of the benzyloxymethyl group (**7c**) largely enhanced the activity (EC_{50}: 0.27 ng/mL), although this conversion resulted in an increase of cytotoxicity compared with **7a** (entry 6). On the other hand, simple 12-ethyl ether (**7d**)

Table 3. Influence of plasma pretreatment on anti-HIV activity of compounds **3** and **7a**

Compound	Plasma	Anti-HIV activity[a] (%)
3	–	100
	+	60.2
7a	–	100
	+	100

[a] These values indicate percentages of the activity based on the plasma (–) values as 100% for each compound at the dose of 100 ng/mL.

exhibited considerably decreased inhibitory activity (entry 7, ca. two-order lower than **7a**). These results clearly suggest that the α-oxyalkyl side chain (acetal structure) at the 12-position plays an important role in exhibiting the effective anti-HIV-1 activity. In addition, the compound **8** with methyl group on the 20-OH group showed lower activity than **7a** (entry 8). Parent compounds (**1** and **2**) exhibited no inhibitory activity against HIV-1 (entries 1 and 2), which is consistent with the previously reported findings.[9] Thus, among the compounds having the ethereal substituent at the 12-position examined in this study, compound **7a** was found to be the most effective phorbol derivative as a new anti-HIV agent in terms of potency, cytotoxicity, and stability against degradation in plasma.

3. Conclusion

In this study, we synthesized and evaluated a new series of 12-*O*-alkylphorbol 13-decanoate, aiming at the discovery of new effective anti-HIV agents with in vivo efficacy. As a result of in vitro screening of the bioactivity, 12-*O*-(methoxymethyl)phorbol 13-decanoate (**7a**) was newly found to exhibit high potency and low cytotoxicity, resulting in a good safety index. Moreover, this compound was demonstrated to keep its anti-HIV-1 activity even after pre-incubation with mouse plasma, implying that it has sufficient stability under physiological conditions in contrast to the corresponding 12-acetate (**3**). Further exploration to find more efficient phorbol derivatives with an in-depth in vivo assay is

Table 2. Anti-HIV activity and safety index of new phorbol derivatives

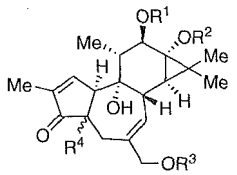

Entry		R^1	R^2	R^3	R^4	Anti-HIV activity (EC_{50}, ng/mL)	Cytotoxicity (CC_{50}, μg/mL)	Safety index (CC_{50}/EC_{50})
1	**1**	H	H	H	β-OH	>10,000	>10,000	—
2	**2**	H	H	H	α-OH	>10,000	>10,000	—
3	**3**	Ac	Decanoyl	H	β-OH	1.7	3.3	1941
4	**7a**	MOM	Decanoyl	H	β-OH	1.3	8.3	6385
5	**7b**	MEM	Decanoyl	H	β-OH	3.72	3.3	887
6	**7c**	BOM	Decanoyl	H	β-OH	0.27	4.4	16,296
7	**7d**	Et	Decanoyl	H	β-OH	195.7	3.3	17
8	**8**	MOM	Decanoyl	Me	β-OH	46.9	4.0	85

ongoing in the search for new clinically useful anti-HIV agents.

4. Experimental

4.1. Chemistry

All nonaqueous reactions were carried out under an Ar atmosphere. Reagents were purchased from commercial sources and used as received. Anhydrous solvents were obtained from commercial sources or prepared by distillation over CaH_2 or P_2O_5. ^1H and ^{13}C NMR spectra were obtained on a Varian Gemini 300 (300 MHz for ^1H and 75.46 MHz for ^{13}C) instrument or a Varian UNITY plus 500 (500 MHz for ^1H and 125 MHz for ^{13}C) instrument, using tetramethylsilane or chloroform as an internal reference. Mass spectra were measured on a JEOL D-200 or a JEOL AX 505 mass spectrometer, and the ionization method was electron impact (EI, 70 eV). IR spectra were recorded on a Perkin–Elmer 1600 spectrometer. The optical rotations were determined on a JASCO DIP-1000 instrument. Melting points were taken with a Yanagimoto micro-melting point apparatus and are uncorrected. Column chromatography was carried out by employing Cica Silica Gel 60N (spherical, neutral, 40–50 or 63–210 μm). Phorbol (**1**) and isophorbol (**2**) were obtained by reported procedure.[10] 12-*O*-Acetylphorbol 13-decanoate (**3**) was identified with the reported one.[12]

4.1.1. 20-*O*-(*tert*-Butyldimethylsilyl)phorbol (4). To a solution of phorbol (**1**, 364 mg, 1 mmol), *N*,*N*-dimethylaminopyridine (12 mg, 0.1 mmol), and imidazole (201 mg, 3 mmol) in DMF (2 mL) at 0 °C was added *tert*-butyldimethylsilyl chloride (166 mg, 1.1 mmol). The solution was stirred for 1 h at room temperature and the mixture was directly subjected to column chromatography on silica gel (AcOEt). The collected fractions were concentrated and the residue containing DMF was dissolved in CH_2Cl_2–hexane (1:1) and then cooled. The precipitates formed were collected by filtration and dried to afford **1** (292 mg, 61%) as a colorless solid. Mp 270–273 °C (decomp.); ^1H NMR (acetone-d_6): δ 0.07 (3H, s), 0.08 (3H, s), 0.71 (1H, d, J = 5.2 Hz), 0.89 (9H, s), 1.06 (3H, d, J = 6.3 Hz), 1.15 (3H, s), 1.26 (3H, s), 1.69 (3H, dd, J = 3.0, 1.3 Hz), 1.95–2.00 (1H, m), 2.46 (2H, s), 3.09–3.14 (2H, m), 3.24 (1H, br s), 3.51 (1H, br), 4.05 (2H, s), 4.09 (1H, br), 4.10 (1H, d, J = 9.8 Hz), 4.65 (1H, s), 5.61 (1H, d, J = 5.6 Hz), 7.58 (1H, s); ^{13}C NMR (acetone-d_6): δ −5.1, 10.2, 15.5, 17.8, 18.8, 24.1, 26.2, 26.5, 37.2, 38.3, 40.1, 46.1, 58.2, 63.0, 68.6, 74.5, 78.8, 81.4, 130.3, 133.1, 140.9, 159.8, 208.5; IR (KBr) cm^{-1}: 3315, 1675. Anal. Calcd for $C_{26}H_{42}O_6Si$: C, 65.24; H, 8.84. Found: C, 64.95; H, 8.69; MS *m*/*z* 478 (M^+−*t*-Bu); HRMS Calcd for $C_{22}H_{33}O_6Si$: 421.2046 (M^+−*t*-Bu). Found: 421.2027; $[\alpha]_D^{25}$ +83.39 (*c* 0.85, MeOH).

4.1.2. 20-*O*-(*tert*-Butyldimethylsilyl)phorbol 13-decanoate (5). To a solution of **4** (48 mg, 0.1 mmol) and triethylamine (42 μL, 0.3 mmol) in CH_2Cl_2 (1 mL) at 0 °C was added decanoyl chloride (41 μL, 0.2 mmol), and the mixture was stirred at room temperature for 3 h. The reaction mixture was diluted with CH_2Cl_2 and washed with 10% HCl, saturated aqueous $NaHCO_3$, and brine, then dried over $MgSO_4$. The solvent was evaporated off to leave a residue, which was chromatographed on silica gel (CH_2Cl_2–AcOEt = 4:1) to afford **5** (47 mg, 74%) as a colorless oil. ^1H NMR ($CDCl_3$): δ 0.04 (3H, s), 0.05 (3H, s), 0.87 (3H, t, J = 6.8 Hz), 0.88 (9H, s), 0.99 (1H, d, J = 5.6 Hz), 1.03 (3H, d, J = 6.8 Hz), 1.19 (3H, s), 1.23 (3H, s), 1.22–1.36 (12H, m), 1.58–1.65 (2H, m), 1.76 (3H, dd, J = 3.0, 1.3 Hz), 1.97–2.04 (1H, m), 2.33–2.37 (3H, m), 2.46 (1H, d, J = 19 Hz), 2.71 (1H, s), 3.13 (2H, br), 3.96 (1H, d, J = 9.8 Hz), 4.00 (2H, s), 5.59 (1H, d, J = 5.8 Hz), 7.56 (1H, d, J = 1.3 Hz); ^{13}C NMR ($CDCl_3$): δ −5.3, 10.1, 14.1, 15.1, 16.9, 18.4, 22.6, 23.7, 24.8, 25.8, 25.9, 26.6, 29.1, 29.20, 29.22, 29.4, 31.8, 34.3, 35.5, 38.3, 39.0, 44.9, 56.8, 67.9, 73.5, 77.5, 78.2, 127.6, 132.9, 140.5, 160.4, 176.9, 209.0; IR (neat) cm^{-1}: 3396, 1706; MS *m*/*z* 575 (M^+−*t*-Bu); HRMS Calcd for $C_{32}H_{51}O_7Si$: 575.3404 (M^+−*t*-Bu). Found: 575.3432; $[\alpha]_D^{25}$ +65.95 (*c* 0.71, $CHCl_3$).

4.1.3. General procedure for the synthesis of 20-*O*-(*tert*-butyldimethylsilyl)-12-*O*-(α-oxyalkyl)phorbol 13-decanoate (6a–c). To a solution of **5** and *N*,*N*-diisopropylethylamine (2 equiv) in CH_2Cl_2 was added chloromethyl methyl ether, chloromethyl 2-methoxyethyl ether, or benzyloxymethyl chloromethyl ether (1.2 equiv) at 0 °C, and the mixture was stirred at room temperature for 20 h. The mixture was diluted with CH_2Cl_2 and washed with 10% HCl, saturated aqueous $NaHCO_3$, and brine, then dried over $MgSO_4$. Removal of the solvent left a residue, which was chromatographed on silica gel (CH_2Cl_2–AcOEt = 9:1) to afford **6a** (63%), **6b** (63%), or **6c** (48%) as a colorless oil, respectively. Compound **6a**: ^1H NMR ($CDCl_3$): δ 0.04 (3H, s), 0.05 (3H, s), 0.87 (9H, s), 0.88 (3H, t, J = 6.8 Hz), 0.97 (1H, d, J = 5.6 Hz), 1.05 (3H, d, J = 6.4 Hz), 1.18 (3H, s), 1.24 (3H, s), 1.22–1.33 (12H, m), 1.60–1.66 (2H, m), 1.77 (3H, dd, J = 3.0, 1.3 Hz), 2.02–2.07 (1H, m), 2.18 (1H, s), 2.32 (2H, td, J = 7.7, 2.6 Hz), 2.39 (1H, d, J = 19 Hz), 2.46 (1H, d, J = 19 Hz), 3.12 (1H, t, J = 5.6 Hz), 3.23 (1H, br s), 3.36 (3H, s), 3.94 (1H, d, J = 9.4 Hz), 4.00 (2H, s), 4.54 (1H, d, J = 6.8 Hz), 4.88 (1H, d, J = 6.8 Hz), 5.61 (1H, d, J = 6.3 Hz), 5.65 (1H, s), 7.61 (1H, s); ^{13}C NMR ($CDCl_3$): δ −5.30, −5.28, 10.1, 14.1, 15.2, 16.8, 18.4, 22.6, 23.8, 24.6, 25.6, 25.9, 29.1, 29.23, 29.24, 29.4, 31.8, 34.5, 36.1, 38.4, 39.1, 44.2, 55.7, 56.1, 65.6, 68.2, 73.7, 77.8, 79.8, 95.0, 128.5, 132.4, 139.9, 161.2, 176.2, 209.2; IR (neat) cm^{-1}: 3404, 1709; MS *m*/*z* 676 (M^+); HRMS Calcd for $C_{38}H_{64}O_8Si$: 676.4370 (M^+). Found: 676.4402; $[\alpha]_D^{25}$ +78.75 (*c* 0.53, $CHCl_3$). Compound **6b**: ^1H NMR ($CDCl_3$): δ 0.02 (6H, s), 0.81–0.90 (12H, m), 0.94 (1H, d, J = 5.6 Hz), 0.98 (3H, d, J = 6.3 Hz), 1.13 (3H, s), 1.15–1.30 (15H, m), 1.57–1.68 (2H, m), 1.72 (3H, d, J = 1.4 Hz), 1.98–2.05 (1H, m), 2.29–2.35 (2H, m), 2.37 (1H, d, J = 19 Hz), 2.40 (1H, d, J = 19 Hz), 2.72 (1H, br), 3.08 (1H, br), 3.17 (1H, br), 3.35 (3H, s), 3.46–3.55 (2H, m), 3.61–3.75 (2H, m), 3.94 (1H, d, J = 9.6 Hz), 3.97 (2H, s), 4.64 (1H, d, J = 6.6 Hz), 4.94 (1H, d, J = 6.6 Hz), 5.57 (1H, d, J = 4.1 Hz), 5.60 (1H, s), 7.55 (1H, s); ^{13}C NMR ($CDCl_3$): δ −5.0, 10.3, 14.3, 15.4,

17.1, 18.6, 22.9, 24.0, 24.8, 25.8, 26.2, 29.3, 29.5, 29.6, 32.0, 34.7, 36.3, 38.5, 39.3, 44.3, 56.3, 59.1, 65.6, 67.2, 68.3, 71.8, 73.8, 77.9, 80.1, 93.8, 128.4, 132.5, 140.0, 160.9, 176.1, 209.0; IR (neat) cm^{-1}: 3411, 1711; MS *m/z* 720 (M^+); HRMS Calcd for $C_{40}H_{68}O_9Si$: 720.4633 (M^+). Found: 720.4622; $[\alpha]_D^{25}$ +79.98 (*c* 0.90, $CHCl_3$). Compound **6c**: ^1H NMR ($CDCl_3$): δ 0.04 (3H, s), 0.05 (3H, s), 0.82–0.92 (12H, m), 0.98 (1H, d, J = 5.2 Hz), 1.05 (3H, d, J = 6.3 Hz), 1.20 (3H, s), 1.20–1.32 (15H, m), 1.50–1.58 (2H, m), 1.75 (3H, d, J = 1.6 Hz), 2.02–2.15 (1H, m), 2.21 (2H, t, J = 7.7 Hz), 2.41 (1H, d, J = 19 Hz), 2.45 (1H, d, J = 19 Hz), 2.63 (1H, br), 3.12 (1H, br), 3.22 (1H, br s), 4.00 (2H, s), 4.05 (1H, d, J = 9.6 Hz), 4.58 (1H, d, J = 11 Hz), 4.65 (1H, d, J = 11 Hz), 4.72 (1H, d, J = 6.9 Hz), 5.01 (1H, d, J = 6.9 Hz), 5.61 (1H, d, J = 5.5 Hz), 5.65 (1H, s), 7.25–7.38 (5H, m), 7.59 (1H, s); ^{13}C NMR ($CDCl_3$): δ −4.9, 10.4, 14.4, 15.5, 17.2, 18.6, 22.9, 24.1, 24.8, 25.8, 26.2, 29.3, 29.4, 29.5, 29.6, 32.1, 34.7, 36.4, 38.6, 39.4, 44.4, 56.3, 65.6, 68.3, 69.8, 73.9, 77.9, 80.3, 93.2, 127.7, 127.8, 128.4, 128.5, 132.5, 138.0, 140.0, 161.0, 176.2, 209.0; MS *m/z* 751 (M^+−H); HRMS Calcd for $C_{44}H_{67}O_8Si$: 751.4605 (M^+−H). Found: 751.4603.

4.1.4. 12-*O*-Ethyl-20-*O*-(*tert*-butyldimethylsilyl)phorbol 13-decanoate (6d). To a solution of **5** (275 mg, 0.43 mmol) and 2,6-di-*tert*-butyl-4-methylpyridine (356 mg, 1.74 mmol) in CH_2Cl_2 (4 mL) was added ethyl trifluoromethanesulfonate (0.13 mL, 1.04 mmol) at 0 °C. The reaction was continued for 65 h at room temperature and quenched with H_2O. After diluting with CH_2Cl_2, the organic layer was washed with saturated aqueous $NaHCO_3$ and brine, successively, and dried over $MgSO_4$. The solvent was evaporated to leave a residue, which was chromatographed on silica gel (CH_2Cl_2–AcOEt = 4:1) to afford **6d** (28 mg, 10%) as a colorless oil. ^1H NMR ($CDCl_3$): δ 0.05 (6H, s), 0.81–0.96 (13H, m), 1.01 (3H, d, J = 6.6 Hz), 1.11–1.18 (3H, m), 1.13 (3H, s), 1.22 (3H, s), 1.20–1.39 (12H, m), 1.58–1.70 (2H, m), 1.78 (3H, s), 1.98–2.03 (1H, m), 2.22–2.38 (3H, m), 2.43 (1H, d, J = 19 Hz), 2.61 (1H, br), 3.17 (1H, br), 3.27–3.38 (1H, m), 3.39–3.49 (2H, m), 3.99 (3H, br s), 4.28 (1H, s), 5.61 (1H, d, J = 3.3 Hz), 7.47 (1H, s); ^{13}C NMR ($CDCl_3$): δ −4.9, 10.5, 14.4, 16.0, 16.1. 17.5, 18.7, 23.0, 23.6, 25.3, 26.2, 27.5, 29.4, 29.5, 29.7, 30.4, 32.1, 34.4, 35.3, 38.5, 39.0, 46.5, 49.7, 59.4, 68.2, 69.7, 73.7, 78.6, 83.7, 128.8, 133.6, 137.5, 160.6, 177.7, 209.0; IR (neat) cm^{-1}: 3419, 1711; MS *m/z* 659 (M^+−H); HRMS Calcd for $C_{38}H_{63}O_7Si$: 659.4343 (M^+−H). Found: 659.4383; $[\alpha]_D^{25}$ +81.97 (*c* 0.120, $CHCl_3$).

4.1.5. General procedure for the synthesis of 12-*O*-alkyl or 12-*O*-(α-oxyalkyl)phorbol 13-decanoate (7a–d). To a solution of **6** in THF was added tetra-*n*-butylammonium fluoride (1 M solution in THF; 2 equiv) at 0 °C, and the solution was stirred for 1.5 h at room temperature. Saturated aqueous NH_4Cl was added to the reaction mixture, and the aqueous solution was extracted with $CHCl_3$ and dried over $MgSO_4$. Removal of the solvent left a residue, which was chromatographed on silica gel (CH_2Cl_2–AcOEt = 4:1) to afford **7a** (94%), **7b** (72%), **7c** (94%), and **7d** (75%) as a colorless oil, respectively. Compound **7a**: ^1H NMR ($CDCl_3$): δ 0.88 (3H, t, J = 7.3 Hz), 1.00 (1H, d, J = 5.6 Hz), 1.06 (3H, d, J = 6.8 Hz), 1.19 (3H, s), 1.22–1.35 (15H, m), 1.59–1.62 (2H, m), 1.78 (3H, d, J = 1.7 Hz), 2.02–2.07 (1H, m), 2.24 (1H, s), 2.29–2.35 (2H, td, J = 7.7, 3.4 Hz), 2.46 (1H, d, J = 19 Hz), 2.53 (1H, d, J = 19 Hz), 3.18 (1H, t, J = 5.6 Hz), 3.23 (1H, s), 3.36 (3H, s), 3.94 (1H, d, J = 9.8 Hz), 3.98 (1H, d, J = 13 Hz), 4.04 (1H, d, J = 13 Hz), 4.54 (1H, d, J = 6.8 Hz), 4.88 (1H, d, J = 6.8 Hz), 5.67 (1H, d, J = 4.7 Hz), 5.76 (1H, s), 7.61 (1H, s); ^{13}C NMR ($CDCl_3$): δ 10.4, 14.4, 15.4, 17.1, 22.9, 24.1, 24.8, 25.8, 29.1, 29.3, 29.5, 29.6, 32.1, 34.8, 36.3, 38.7, 39.2, 44.3, 55.9, 56.2, 65.7, 68.1, 73.8, 78.2, 79.9, 95.1, 129.3, 132.7, 140.6, 160.9, 176.3, 209.1; IR (neat) cm^{-1}: 3409, 1709; MS *m/z* 501 (M^+−OCH_2OCH_3); HRMS Calcd for $C_{30}H_{45}O_6$: 501.3216 (M^+−OCH_2OCH_3). Found: 501.3200; $[\alpha]_D^{25}$ +89.27 (*c* 0.11, $CHCl_3$). Compound **7b**: ^1H NMR ($CDCl_3$): δ 0.86 (3H, t, J = 7.1 Hz), 0.98 (1H, d, J = 5.6 Hz), 1.00 (3H, d, J = 6.8 Hz), 1.16 (3H, s), 1.21 (3H, s), 1.21–1.35 (12H, m), 1.55–1.63 (2H, m), 1.72 (3H, d, J = 1.4 Hz), 2.00–2.10 (1H, m), 2.31 (2H, td, J = 7.4, 2.5 Hz), 2.44 (1H, d, J = 19 Hz), 2.51 (1H, d, J = 19 Hz), 3.05–3.19 (3H, m), 3.36 (3H, s), 3.52 (2H, t, J = 4.9 Hz), 3.60–3.75 (2H, m), 3.90–4.02 (3H, m), 4.65 (1H, d, J = 6.9 Hz), 4.94 (1H, d, J = 6.9 Hz), 5.63 (1H, d, J = 5.2 Hz), 5.75 (1H, s), 7.55 (1H,s); ^{13}C NMR ($CDCl_3$): δ 10.4, 14.4, 15.5, 17.1, 22.9, 24.1, 24.8, 25.8, 29.4, 29.5, 29.6, 32.1, 34.8, 36.3, 38.7, 39.2, 44.3, 56.3, 59.2, 65.7, 67.3, 68.2, 71.9, 73.8, 78.2, 80.1, 94.0, 129.3, 132.7, 140.5, 161.0, 176.3, 209.1; IR (neat) cm^{-1}: 3406, 1709; MS *m/z* 606 (M^+); HRMS Calcd for $C_{34}H_{54}O_9$: 606.3768 (M^+). Found: 606.3779; $[\alpha]_D^{25}$ +85.88 (*c* 1.00, $CHCl_3$). Compound **7c**: ^1H NMR ($CDCl_3$): 0.87 (3H, t, J = 6.9 Hz), 1.01 (1H, d, J = 5.2 Hz), 1.06 (3H, d, J = 6.1 Hz), 1.11–1.36 (18H, m), 1.45–1.60 (2H, m), 1.73 (3H, s), 2.02–2.15 (1H, m), 2.20 (2H, t, J = 7.4 Hz), 2.46 (1H, d, J = 19 Hz), 2.54 (1H, d, J = 19 Hz), 3.20 (3H, br), 3.90–4.04 (3H, m), 4.56 (1H, d, J = 12 Hz), 4.64 (1H, d, J = 12 Hz), 4.71 (1H, d, J = 6.9 Hz), 4.99 (1H, d, J = 6.9 Hz), 5.66 (1H, d, J = 5.5 Hz), 5.81 (1H, s), 7.22–7.37 (5H, m), 7.58 (1H, s); ^{13}C NMR ($CDCl_3$): δ 10.4, 14.4, 15.5, 17.2, 22.9, 24.1, 24.8, 25.9, 29.3, 29.4, 29.5, 29.6, 32.1, 34.7, 36.3, 38.7, 39.2, 44.4, 56.2, 65.6, 68.2, 69.8, 73.8, 78.3, 80.3, 93.2, 127.7, 127.8, 128.4, 129.4, 132.7, 137.9, 140.6, 161.0, 176.4, 209.2; IR (neat) cm^{-1}: 3399, 1708; MS *m/z* 638 (M^+); $[\alpha]_D^{25}$ +70.75 (*c* 3.45, $CHCl_3$). Compound **7d**; ^1H NMR ($CDCl_3$): 0.82–0.95 (4H, m), 1.03 (3H, d, J = 6.6 Hz), 1.13–1.17 (6H, m), 1.20–1.39 (15H, m), 1.59–1.70 (2H, m), 1.78 (3H, d, J = 1.6 Hz), 1.95–2.07 (2H, m), 2.30–2.41 (3H, m), 2.50 (1H, d, J = 19 Hz), 2.97 (1H, br s), 3.17 (1H, br), 3.25–3.37 (1H, m), 3.40–3.49 (2H, m), 3.97–4.03 (3H, m), 4.30 (1H, s), 5.63 (1H, br s), 7.48 (1H, s); ^{13}C NMR ($CDCl_3$): δ 10.5, 14.4, 15.9, 16.1, 17.6, 23.0, 23.6, 25.3, 25.9, 27.5, 29.4, 29.5, 29.7, 32.1, 34.4, 35.2, 38.6, 39.1, 46.5, 49.7, 59.4, 68.4, 69.6, 73.7, 78.7, 83.7, 130.1, 133.9, 138.1, 160.6, 177.7, 209.2; IR (neat) cm^{-1}: 3449, 1708; MS *m/z* 546 (M^+); HRMS Calcd for $C_{32}H_{50}O_7$: 546.3557 (M^+). Found: 546.3548; $[\alpha]_D^{25}$ +109.81 (*c* 0.745, $CHCl_3$).

4.1.6. 12-*O*-Methoxymethyl-20-*O*-methylphorbol 13-decanoate (8). According to the procedure for the synthesis of **6d**, the compound **7a** (49 mg, 0.087 mmol)

was treated with 2,6-di-*tert*-butyl-4-methylpyridine and methyl trifluoromethanesulfonate to afford **8** (44 mg, 88%) as a colorless oil. ^{1}H NMR ($CDCl_3$): δ 0.87 (3H, t, J = 7.1 Hz), 0.99 (1H, d, J = 5.2 Hz), 1.03 (3H, d, J = 6.3 Hz), 1.17 (3H, s), 1.18–1.35 (15H, m), 1.55–1.68 (2H, m), 1.75 (3H, t, J = 1.4 Hz), 2.00–2.10 (1H, m), 2.32 (2H, t, J = 7.4 Hz), 2.44 (1H, d, J = 19 Hz), 2.48 (1H, d, J = 19 Hz), 2.57 (1H, br), 3.14–3.24 (2H, m), 3.27 (3H, s), 3.36 (3H, s), 3.73 (1H, d, J = 12 Hz), 3.81 (1H, d, J = 12 Hz), 3.93 (1H, d, J = 9.6 Hz), 4.54 (1H, d, J = 6.7 Hz), 4.88 (1H, d, J = 6.7 Hz), 5.63 (1H, s), 5.66 (1H, s), 7.58 (1H, s); ^{13}C NMR ($CDCl_3$): δ 10.4, 14.4, 15.4, 17.1, 22.9, 24.1, 24.8, 25.8, 29.4, 29.5, 29.6, 32.1, 34.8, 36.3, 39.1, 39.5, 44.4, 55.9, 56.4, 58.2, 65.7, 73.8, 78.1, 80.0, 95.2, 131.3, 132.7, 137.6, 161.0, 176.2, 209.0; IR (neat) cm^{-1}: 3411, 1710; MS *m/z* 576 (M^+); HRMS Calcd for $C_{33}H_{52}O_8$: 576.3662 (M^+). Found: 576.3613; $[\alpha]_D^{25}$ +103.53 (*c* 2.00, $CHCl_3$).

4.2. Biology

4.2.1. Preparation of the test compound solutions. The test compounds were dissolved in DMSO and then diluted with physiological saline or medium solution. In the stability test, the test compounds were diluted with plasma collected from male BALB/cA mice and the mixed solutions were incubated on the water bath at 37 °C for 30 min. The plasma was prepared with 3.8% sodium citrate added blood, collected from the inferior vena cava.

4.2.2. Cells and virus. T-cell lines MT-4 and Molt-4 cells, and the HIV-1 IIIB infected Molt-4 cells, were grown in RPMI 1640 medium supplemented with 10% fetal bovine serum (Cansera international Inc., Canada) and antibiotics (100 μg/mL penicillin/100 μg/mL streptomycin). HIV-1 IIIB viral stocks were prepared by propagation in co-culturing of HIV-1 IIIB infected Molt-4 and uninfected Molt-4 cells.

4.2.3. MTT assay. To determine susceptibility to HIV-1 and cytotoxicity, MT-4 cells were infected with HIV-1 IIIB strains at multiplicity of infection (MOI) of 0.01, and infected or uninfected MT-4 cells (mock infection) were cultured in the presence or absence of serial concentrations of the test compounds for 5 days. Cell viability was quantified with 3-(4,5-dimethylthiazol-2-yl)-3,5-diphenylformazan (MTT, Dojindo, Japan) assay. The absorbances were read at two wavelengths (540 and 690 nm). All data were calculated using the median OD (optical density) value of three wells. The concentration achieving 50% protection in HIV-1 infected cells was determined as the 50% effective concentration (EC_{50}) for drug susceptibility, and 50% cytotoxic concentration (CC_{50}) values were calculated at uninfected cells for drug cytotoxicity.

Supplementary data

Supplementary data associated with this article can be found in the online version at doi:10.1016/j.bmc.2005.04.056.

References and notes

1. (a) Che, C.-T. In *Economic and Medical Plant Research*; Wagner, H., Farnsworth, N. R., Eds.; Academic: London, UK, 1991; Vol. 5; (b) Kusumoto, I. T.; Hattori, M. In *Pharmacological Research on Traditional Herbal Medicines*; Watanabe, H., Sibuya, T., Eds.; Harwood Academic: Amsterdam, 1999, pp 219–235; (c) Schinazi, R. F. In *Natural Products as Antiviral Agents*; Chu, C.-K., Cutler, H. G., Eds.; Plenum: New York, 1992, pp 1–29; (d) Nasr, M.; Cradock, J.; Johnson, M. In *Natural Products as Antiviral Agents*; Chu, C.-K., Cutler, H. G., Eds.; Plenum: New York, 1992, pp 31–56; (e) Ng, T. B.; Huang, B.; Fong, W. P.; Yeung, H. W. *Life Sci.* **1997**, *61*, 933; (f) El-Mekkawy, S.; Meselhy, M. R.; Kusumoto, I. T.; Kadota, S.; Hattori, M.; Namba, T. *Chem. Pharm. Bull.* **1995**, *43*, 641; (g) El-Mekkawy, S.; Meselhy, M. R.; Nakamura, N.; Tezuka, Y.; Hattori, M.; Kakiuchi, N.; Shimotohno, K.; Kawahata, T.; Otake, T. *Phytochemistry* **1998**, *49*, 1651.
2. (a) El-Mekkawy, S.; Meselhy, M. R.; Nakamura, N.; Hattori, M.; Kawahata, T.; Otake, T. *Chem. Pharm. Bull.* **1999**, *47*, 1346; (b) El-Mekkawy, S.; Meselhy, M. R.; Nakamura, N.; Hattori, M.; Kawahata, T.; Otake, T. *Phytochemistry* **2000**, *53*, 457.
3. See, for example (a) Evans, F. J.; Taylor, S. E. In *Progress in the Organic Chemistry of Natural Products*; Herz, W., Grisebach, H., Kirby, G. W., Eds.; Springer: New York, 1983; Vol. 44, pp 1–99; (b) Dicker, P.; Rozengurt, E. *Nature* **1980**, *287*, 607; (c) Billah, M. M.; Lapetina, E. G.; Cuatrecasas, P. *J. Biol. Chem.* **1981**, *256*, 5399; (d) De Chaffoy de Courcelles, D.; Roevens, P.; van Belle, H. *FEBS Lett.* **1984**, *173*, 389; (e) Acres, R. B.; Conlon, P. J.; Mochizuki, D. Y.; Gallis, B. *J. Biol. Chem.* **1986**, *261*, 16210.
4. See, for example, (a) Kishi, Y.; Rando, R. R. *Acc. Chem. Res.* **1998**, *31*, 163; (b) Nishizuka, Y. *Nature* **1988**, *334*, 661; (c) Nishizuka, Y. *Nature* **1984**, *308*, 693; (d) Blumberg, P. M.; Dunn, J. A.; Jaken, S.; Jeng, A.; Leach, K. L.; Sharkey, N. A.; Yeh, E. In *Mechanism of Tumor Promotion*; Slaga, T. J., Ed.; Tumor Promotion and Cocarcinogenesis In Vitro; CRC: Boca Raton, 1984; Vol. 3, pp 143–184; (e) Blumberg, P. M. *CRC Crit. Rev. Toxicol.* **1981**, *8*, 153; (f) Blumberg, P. M. *CRC Crit. Rev. Toxicol.* **1981**, *8*, 199.
5. (a) Yeh, E.; Sharkey, N. A.; Blumberg, P. M. *Phytother. Res.* **1987**, *1*, 135; (b) Kubinyi, H. *Arzneim. Forsch.* **1976**, *26*, 1991.
6. Wada, R.; Suto, Y.; Kanai, M.; Shibasaki, M. *J. Am. Chem. Soc.* **2002**, *124*, 10658.
7. Chowdhury, M. I.; Koyanagi, Y.; Kobayashi, S.; Hamamoto, Y.; Yoshiyama, H.; Yoshida, T.; Yamamoto, N. *Virology* **1990**, *176*, 126.
8. Gustafson, K. R.; Cardellina, J. H., II; McMahon, J. B.; Gulakowski, R. J.; Ishitoya, J.; Szallasi, Z.; Lewin, N. E.; Blumberg, P. M.; Weislow, O. S.; Beutler, J. A.; Buckheit, R. W., Jr.; Cragg, G. M.; Cox, P. A.; Bader, J. P.; Boyd, M. R. *J. Med. Chem.* **1992**, *35*, 1978.
9. El-Mekkawy, S.; Meselhy, M. R.; Abdel-Hafez, A. A.-M.; Nakamura, N.; Hattori, M.; Kawahata, T.; Otake, T. *Chem. Pharm. Bull.* **2002**, *50*, 523.
10. (a) Cairnes, D. A.; Mirvish, S. S.; Wallcave, L.; Nagel, D. L.; Smith, J. W. *Cancer Lett.* **1981**, *14*, 85; (b) Mishra, N. C.; Estensen, R. D.; Abdel-Monem, M. M. *J. Chromatogr.* **1986**, *369*, 435.
11. Sorg, B.; Fürstenberger, G.; Berry, D. L.; Hecker, E.; Marks, F. *J. Lipid Res.* **1982**, *23*, 443.
12. Hecker, E. In *Methods of Cancer Research*; Busch, H., Ed.; Academic: London, UK, 1971; Vol. 6, pp 439–481.

AIDS RESEARCH AND HUMAN RETROVIRUSES
Volume 21, Number 11, 2005, pp. 977–980

Sequence Note

Molecular Epidemiology of the Heterosexual HIV-1 Transmission in Kunming, Yunnan Province of China Suggests Origin from the Local IDU Epidemic

XIAO-JIE LI,[1,2] SHIGERU KUSAGAWA,[1] XUESHAN XIA,[3] CHAOJUN YANG,[1,4] QIANQIU WANG,[1,2] YUKO YOKOTA,[1] YOSHIMI HOSHINA,[1] TOSHINARI ONOGI,[1] KYOKO NOHTOMI,[1] YUKO IMAMURA,[1] TEIICHIRO SHIINO,[1] RONGGE YANG,[1] NAOKI YAMAMOTO,[1] KUNLONG BEN,[5,6] and YUTAKA TAKEBE[1]

ABSTRACT

Molecular epidemiological investigation was conducted among injecting drug users (IDUs) (n = 11) and heterosexuals (n = 15) in Kunming, Yunnan Province of China. HIV-1 genotypes were determined based on the nucleotide sequences of 2.6-kb *gag*-RT region. The distribution of genotypes among IDUs was as follows: CRF07_BC (5/11) and CRF08_BC (5/11); subtype B′ (1/11). Similarly, a majority of Kunming heterosexuals (14/15) were infected with CRF07_BC (4/15), CRF08_BC (6 /15), or subtype B′ (4/15), known to predominate among IDUs in China. This contrasts with trends in the coastal regions of China and surrounding southeastern Asian countries, where CRF01_AE predominates among heterosexuals. The heterosexual HIV-1 epidemic in Kunming thus appears to derive from the local IDU epidemic. Of note, subtype B′ was the most prevalent strain among heterosexuals before 1997, while CRF07_BC and CRF08_BC became predominant in 2002, indicating a transition of HIV-1 genotype distribution between the early and the more recent samples from Kunming heterosexuals.

THE HIV-1 EPIDEMIC IN CHINA was first detected among injecting drug users (IDUs) in the western part of Yunnan Province in 1989. HIV prevalence among IDUs in initial epidemic sites reached 50–80% by 1993.[1] Yunnan Province accounted for more than 80% of the HIV-1 infections reported in China through 1996[1] and is thought to be an epicenter of the HIV epidemic in China. According to recent HIV-1 sentinel surveys, the HIV-1 prevalence rate among newly tested IDUs in Yunnan has been stable (19.7–24.7% in 1997–1999).[2] However, HIV-1 prevalence rates among female commercial sex workers (CSWs) and wives of heroin users have increased steadily. For example, HIV prevalence among CSWs in Yunnan increased from 1.0% in 1997 to 3.4% in 2001.[2] Figure 1 shows the study site and the geographical distribution of the numbers of HIV reported cases in China as of June 2003 (http://www.aids.net.cn).

HIV-1 strains circulating in Yunnan showed extremely high genetic diversity. Various HIV-1 strains, including subtypes B, B′[3] (Thailand variant of subtype B, also referred to as Thai-B[4]) and C,[5,6] and CRF07_BC and CRF08_BC[7]), have been detected among IDUs. Moreover, in addition to these HIV-1 strains, diverse forms of unique recombinants between subtypes B′ and

[1]Laboratory of Molecular Virology and Epidemiology, AIDS Research Center, National Institute of Infectious Diseases, 1-23-1 Toyama, Shinjuku-ku, Tokyo 162-8640, Japan.
[2]Institute of Dermatology, Chinese Academy of Medical Sciences, 12 Jiangwangmiao Road, Nanjing 210042, The People's Republic of China.
[3]Kunming University of Science and Technology, Kunming, Yunnan 650224, The People's Republic of China.
[4]Yunnan Provincial Health and Anti-epidemic Center, 158 Dongsi Road, Kunming 650022, The People's Republic of China.
[5]Kunming Institute of Zoology, Chinese Academy of Sciences, Kunming, Yunnan 650223, The People's Republic of China.
[6]Kunming Chinaware Biotechnology, Yunnan 650106, The People's Republic of China.

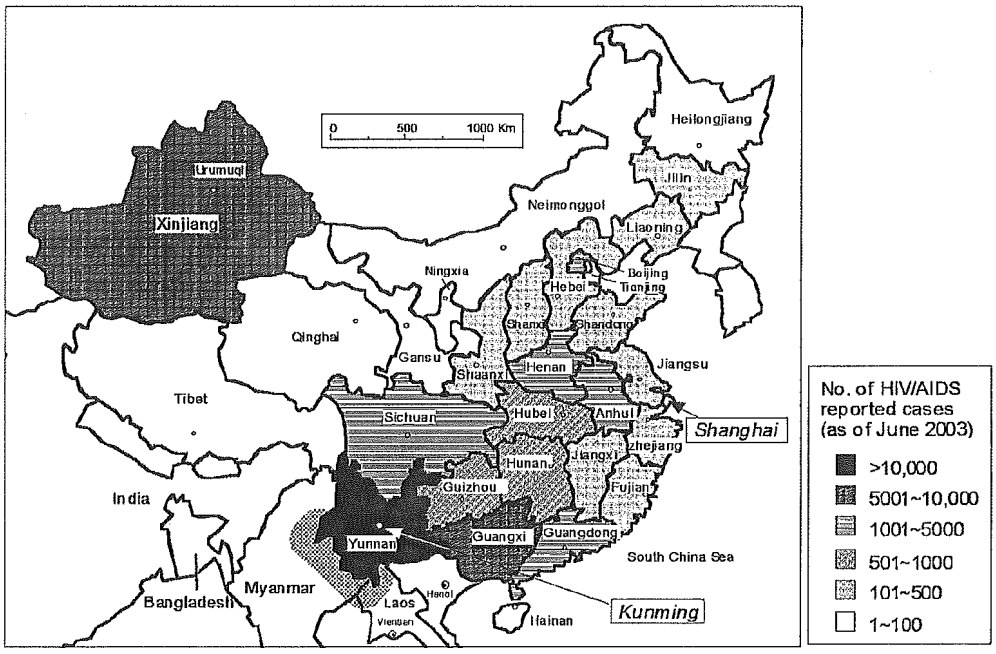

FIG. 1. Map of China. The study site (Kunming, Yunnan Province) and the geographical distribution of the numbers of HIV reported cases (as of June 2003) are shown (http://www.aids.net.cn). The so-called "Golden Triangle," a major heroin production, refining, and trading area, at the borders of Thailand, Myanmar, and Laos, near Yunnan Province, is marked.

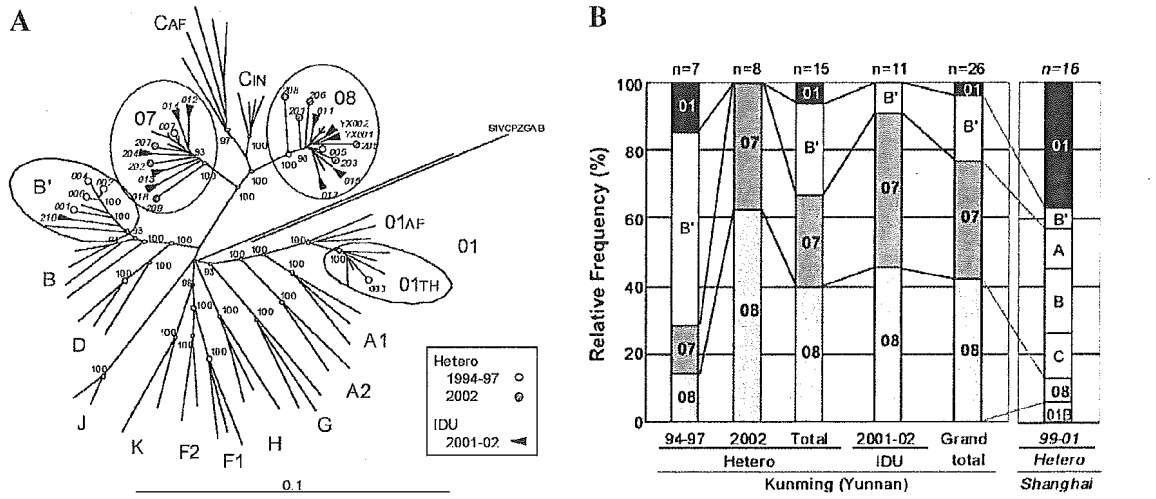

FIG. 2. Phylogenetic tree analysis and the distribution of HIV-1 strains circulating among different risk populations in Kunming, Yunnan. (**A**) Neighbor-joining tree based on the nucleotide sequences of 2.6-kb *gag*-RT regions with HIV-1 group M reference strains (http://hiv-web.lanl.gov/content/hiv-db/SUBTYPE_REF/Table1.html). $SIV_{CPZ}GAB$ was used as an outgroup. Bootstrap values (>90) are shown at the corresponding nodes. Subtype and CRF designations are shown outside the tree. HIV-1 specimens from IDUs were collected in 2001–2002 (closed arrowheads); HIV-1 specimens from heterosexuals sampled in 1994–1997 (open circles) and in 2002 (striped circles). Three-digit numbers indicate the specimen codes. (**B**) Distribution of HIV-1 genotypes in different risk populations. Bars indicate the relative frequency (%) of the indicated HIV-1 genotype in the respective sample category shown at the bottom. The data on HIV-1 genotype distribution among heterosexuals in Shanghai are adopted from Zhong *et al.*[15] *n* indicates the number of the specimens analyzed in each sample category shown below. B′, HIV-1 subtype B′ (Thailand variant of subtype B); C, subtype C; 01, CRF01_AE; 07, CRF07_BC; 08, CRF08_BC; C_{AF}, African subtype C; C_{IN}, Indian subtype C; 01_{AF}, African CRF01_AE; 01_{TH}, Thailand CRF01_AE.

C,[7] and even the second-generation recombinants comprised of CRF07_BC and CRF08_BC,[8] have been reported among IDUs in Yunnan. In contrast, however, information on the HIV-1 genotypes circulating among heterosexuals in Yunnan is very limited. Although an early study detected CRF01_AE in women who had returned from commercial sex work in Thailand[9] and HIV-1 subtype B/B′, C, CRF01_AE, and CRF08_BC have recently been reported in a small number of heterosexuals in Yunnan,[2] HIV-1 genotypes circulating among persons at heterosexual risk have not been well studied. Ongoing monitoring of the HIV-1 genotype distribution in Yunnan would be important for understanding the evolution of the epidemic as well as for future vaccine strategies in China.

To track the HIV-1 genotype distribution in Yunnan, we collected a total of 26 HIV-1-positive plasma samples from persons in the capital city of Kunming and environs during 1994–2002. Fifteen specimens were from persons who acquired HIV-1 infection through heterosexual contact (7 were sampled in 1994–1997 and 8 were collected in 2002). Eleven specimens were collected from IDUs in 2001–2002. The nucleotide sequences of HIV-1 *gag*-RT regions (2.6 kb) were determined on both strands using BigDye terminator reaction kits on an ABI 373 DNA sequencer as described previously.[7] A multiple alignment with HIV-1 group M references (http://hiv-web.lanl.gov/content/hiv-db/SUBTYPE_REF/Table1.html) was generated by the Se-Al program.[10] HIV-1 genotypes were screened and determined based on phylogenetic tree (Fig. 2A) and recombination breakpoint analyses of *gag*-RT regions. Phylogenetic trees were constructed by the neighbor-joining method[11] using PHYLIP package version 3.6a3[12] and the reliability of topologies of trees was tested by bootstrap analysis with 100 bootstrap replicates.[13] Bootscanning analyses were performed on neighbor-joining trees for a window of 200 bp moving along the alignment in 30-bp increments, using the Simplot program.[14]

The distribution of HIV-1 genotypes in a total of 26 samples is as follows (Fig. 2): HIV-1 subtype B′ (Thailand variant of subtype B) (5, 19%); CRF01_AE (1, 4%); CRF07_BC (9, 35%); and CRF08_BC (11, 42%). As shown in Fig. 2B, CRF07_BC (5 of 11, 45%) and CRF08_BC (5 of 11, 45%) are predominantly distributed among IDUs. In contrast, HIV-1 subtype B′ (4 of 7, 57%) was the most common strain among specimens from heterosexuals before 1997, while CRF01_AE, CRF07_BC, and CRF08_BC occurred only infrequently (1 of 7, 14% each). Interestingly, however, CRF07_BC (3 of 8, 38%) and CRF08_BC (5 of 8, 63%) were more common among specimens collected from heterosexuals in 2002, indicating a transition of HIV-1 genotype distribution between the early (before 1997) and the more recent samples (in 2002) from Kunming heterosexuals.

It is noted that the specimens, 208 (02CNKM208) and 209 (02CNKM209), are placed slightly outside the clusters of CRF08_BC and CRF07_BC, respectively (Fig. 2A). The raw direct sequencing data of theses specimens contained several ambiguous signals. The clonal sequence analysis by TA cloning revealed that they were coinfected with another lineage of the HIV-1 strain (X.-J. Li, in preparation).

The small proportion of CRF01_AE among heterosexuals in Kunming (Fig. 2) contrasts with the findings in surrounding Southeast Asian countries, where CRF01_AE shows a strong founder effect triggering the explosive epidemic among heterosexuals.[5] As shown in Fig. 2, it appears that CRF01_AE has not accounted for the majority of sexual transmission in Kunming. Although CRF01_AE was detected in the early 1990s among returnees from Thailand,[9] it has not gained the momentum of dissemination through the sexual route in Kunming, as it has in other Southeast Asian countries. In contrast, CRF01_AE constituted a significant proportion of HIV-1 strains among heterosexuals (6 of 16, 38%) in the city of Shanghai in 1999–2001[15] (Fig.2B. right). This suggests a difference in the structure and the genesis of heterosexual epidemics in Kunming and the coastal areas represented by Shanghai. Heterosexual transmission of HIV-1 in Kunming thus appears to be strongly influenced by the local IDU epidemic, while CRF01_AE shows a significant founder effect among heterosexuals in some coastal regions in China.

In conclusion, the apparent predominance of CRF07_BC and CRF08_BC among heterosexuals in Kunming suggests that a large proportion of these infections are related to IDU networks in China. These findings would contribute to our understanding of the HIV-1 epidemic in China.

ACKNOWLEDGMENTS

We would like to thank Tim Mastro for critical reading of our manuscript and Feng Gao for his advice. We also thank Xinming Li for help in the initial phase of our study and Midori Kawasaki for artwork. This study was supported by grants from the Ministry of Health, Labour and Welfare, Ministry of Education, Science and Technology, and Japanese Foundation for AIDS Prevention (JFAP). X.-J. L. is a recipient of a Research Resident Fellowship from JFAP. C.Y. is a research fellow of the Japan–China Medical Association. Q.W. is a Fellow of the Takeda Science Foundation.

The Genbank accession numbers of the nucleotide sequences reported in this article are AB213667–AB213692.

REFERENCES

1. Zheng X, Tian C, Choi KH, *et al.*: Injecting drug use and HIV infection in southwest China. AIDS 1994;8:1141–1147.
2. Yu XF, Wang X, Mao P, *et al.*: Characterization of HIV type 1 heterosexual transmission in Yunnan, China. AIDS Res Hum Retroviruses 2003;19:1051–1055.
3. Kalish ML, Baldwin A, Raktham S, *et al.*: The evolving molecular epidemiology of HIV-1 envelope subtypes in injecting drug users in Bangkok, Thailand: Implications for HIV vaccine trials. AIDS 1995;9:851–857.
4. Ou CY, Takebe Y, Weniger BG, *et al.*: Independent introduction of two major HIV-1 genotypes into distinct high-risk populations in Thailand. Lancet 1993;341:1171–1174.
5. Weniger BG, Takebe Y, Ou CY, and Yamazaki S: The molecular epidemiology of HIV in Asia. AIDS 1994;8(Suppl. 2):S13–28.
6. Luo CC, Tian C, Hu DJ, Kai M, Dondero T, and Zheng X: HIV-1 subtype C in China. Lancet 1995;345:1051–1052.
7. Yang R, Xia X, Kusagawa S, Zhang C, Ben K, and Takebe Y: Ongoing generation of multiple forms of HIV-1 intersubtype recombinants in the Yunnan Province of China. AIDS 2002;16:1401–1407.

8. Yang R, Kusagawa S, Zhang C, Xia X, Ben K, and Takebe Y: Identification and characterization of a new class of human immunodeficiency virus type 1 recombinants comprised of two circulating recombinant forms, CRF07_BC and CRF08_BC, in China. J Virol 2003;77:685–695.
9. Cheng H, Zhang J, Capizzi J, Young NL, and Mastro TD: HIV-1 subtype E in Yunnan, China. Lancet 1994;344:953–954.
10. Rambaut A: Se-Al (Sequence Alignment Editor) version 1.0 alpha 1. Department of Zoology, University of Oxford, Oxford, 1996.
11. Saitou N and Nei M: The neighbor-joining method: A new method for reconstructing phylogenetic trees. Mol Biol Evol 1987;4: 406–425.
12. Felsenstein J: PHYLIP (Phylogeny Inference Package) version 3.6a3. Department of Genome Sciences, University of Washington, Seattle, 2002.
13. Felsenstein J: Confidence limits on phylogenies: An approach using the bootstrap. Evolution 1985;39:783–791.
14. Ray SC: Simplot for Windows, version 3.2 (distributed by the author via http://www.sray.med.som.jhmi.edu/RaySoft/SimPlot). Johns Hopkins Medical Institutions, Baltimore, MD, 2002.
15. Zhong P, Kang L, Pan Q, *et al.*: Identification and distribution of HIV type 1 genetic diversity and protease inhibitor resistance-associated mutations in Shanghai, P. R. China. J Acquir Immune Defic Syndr 2003;34:91–101.

Address reprint requests to:
Yutaka Takebe
Laboratory of Molecular Virology and Epidemiology
AIDS Research Center
National Institute of Infectious Diseases
Toyama 1-23-1, Shinjuku-ku
Tokyo 162-8640, Japan

E-mail: takebe@nih.go.jp

Available online at www.sciencedirect.com
SCIENCE DIRECT®
Microbes and Infection 7 (2005) 1150–1160
Microbes and Infection
www.elsevier.com/locate/micinf

Original article

A novel role for Vpr of human immunodeficiency virus type 1 as a regulator of the splicing of cellular pre-mRNA

Madoka Kuramitsu [a,b], Chieko Hashizume [a,b], Norio Yamamoto [c], Akihiko Azuma [a], Masakazu Kamata [a], Naoki Yamamoto [c], Yoshimasa Tanaka [b], Yoko Aida [a,b,*]

[a] *Retrovirus Research Unit, RIKEN, 2-1 Hirosawa, Wako, Saitama 351-0198, Japan*
[b] *Graduate School of Life and Environmental Sciences, University of Tsukuba, Tsukuba, Ibaraki 305-8572, Japan*
[c] *Department of Molecular Virology, Bio-Response, Tokyo Medical and Dental University, Bunkyo-ku, Tokyo 113-8519, Japan*

Received 13 March 2005; accepted 21 March 2005

Available online 19 April 2005

Abstract

Vpr, one of the accessory gene products of human immunodeficiency virus type 1 (HIV-1), affects aspects of both viral and cellular proliferation, being involved in long terminal repeat (LTR) activation, arrest of the cell cycle at the G2 phase, and apoptosis. We have discovered a novel role for Vpr as a regulator of the splicing of pre-mRNA both in vivo and in vitro. We found, by RT-PCR and RNase protection analysis, that Vpr caused the accumulation of incompletely spliced forms of *α-globin 2* and *β-globin* pre-mRNAs in cells that had been transiently transfected with a Vpr expression vector. We postulated that this novel effect of Vpr might occur via a pathway that is distinct from arrest of the cell cycle at G2. By analyzing splicing reactions in vitro, we showed that Vpr inhibited the splicing of *β-globin* pre-mRNA in vitro. The splicing of intron 1 of *α-globin 2* pre-mRNA was modestly inhibited by Vpr but the splicing of intron 2 was unaffected. Interestingly, an experimental infection system which utilizes high-titered HIV-1/vesticular stomatitis virus G protein showed that Vpr expressed from an HIV-1 provirus was sufficient to accumulate endogenous *α-globin 2* pre-mRNA. Thus, it is likely that Vpr contributes to selective inhibition of the splicing of cellular pre-mRNA.

Keywords: Human immunodeficiency virus type 1; Vpr; Splicing; Pre-mRNA

1. Introduction

The genome of human immunodeficiency virus type 1 (HIV-1) contains both structural genes, such as *gag*, *pol*, and *env*, and accessory genes, such as *tat*, *rev*, *vif*, *vpr*, *vpu*, and *nef*. The *vpr* gene encodes a protein of 96 amino acids that is incorporated in significant quantities into virions [1,2]. Vpr is a nucleophilic protein with non-classical nuclear localization signals [3,4]. The presence of Vpr in the viral particle facilitates efficient infection of macrophages and other non-dividing cells [5–7] by mediating the active nuclear import of preintegration complexes (PIC) [8,9]. One of the important functions of Vpr is the promotion of growth arrest at the G2/M phase of the cell cycle [10–13]. Indeed, there are sufficient amounts of Vpr in incoming viral particles to induce G2 arrest of the cell cycle even prior to the initiation of the synthesis of viral proteins de novo [14,15]. In addition, G2 arrest enhances viral replication, in part by increasing the activity of the long terminal repeat (LTR) [16]. Other evidence also suggests that Vpr can regulate apoptosis both positively and negatively [17–22]. Vpr has also been reported to produce herniation and disruption of the nuclear envelope, which might be correlated with G2 arrest and suggests the possibility that Vpr might allow PICs to bypass the size restrictions of nuclear pore complexes [23].

Splicing of pre-mRNA is not only a nearly ubiquitous and essential step in gene expression but it is also an important mechanism for the generation of protein diversity and the regulation of gene expression. The splicing reaction is performed by the spliceosome, which consists of five small nuclear ribonucleoprotein (snRNP) complexes, namely, U1, U2, U4, U5, and U6, and a large number of non-snRNPs, which include members of the serine- and arginine-rich (SR)

* Corresponding author. Tel.: +81 48 462 4408; fax: +81 48 462 4399.
E-mail address: aida@riken.jp (Y. Aida).

1286-4579/$ - see front matter © 2005 Elsevier SAS. All rights reserved.
doi:10.1016/j.micinf.2005.03.022

family of proteins. The spliceosome acts, through a multitude of RNA–RNA, RNA–protein and protein–protein interactions, to excise each intron precisely and to join exons in the correct order [24]. In mammalian cells, SR proteins and other splicing factors are present in regions of the nucleus known splicing factor compartments, nuclear speckles, or interchromatin granules, and they appear to function at several steps in gene expression [25]. Several viral proteins have also been shown to regulate the splicing of pre-mRNAs. For example, NS1 of influenza virus [26,27] and ICP27 of herpes simplex virus (HSV) [28–31] were reported to interfere with splicing of cellular pre-mRNA as part of the mechanism for blockage of host protein synthesis. Moreover, it has been proposed that production of unspliced or partially spliced transcripts of HIV-1 and other lentiviruses might be mediated by the action of virus-encoded Rev, which binds to a specific RNA sequence (the Rev-responsive element or RRE). Rev binds viral RNAs that contain an RRE [32,33] and it exports HIV-1 RNA to the cytoplasm in a CRM1-dependent manner [34–36].

In the present study, we discovered a novel role for Vpr of HIV-1. We demonstrated that Vpr inhibits the splicing of cellular pre-mRNA both in vivo and in vitro. In analyses by RT-PCR and RNase protection assays, we showed that Vpr-induced the accumulation of unspliced forms of *α-globin 2* and *β-globin* pre-mRNA. Furthermore, we confirmed that Vpr inhibited pre-mRNA splicing in an in vitro splicing assay using *β-globin* pre-mRNA as the substrate. We also present strong evidence that Vpr contributes to selective inhibition during the splicing of cellular pre-mRNA. In addition, we demonstrated that HIV-1 infection was sufficient to inhibit splicing of *α-globin 2* pre-mRNA using vesicular stomatitis virus G protein (VSV-G) pseudotyped HIV-1 viruses. Our results reveal a novel function of Vpr and contribute to an enhanced understanding of splicing mechanisms and the life cycle of HIV-1.

2. Materials and methods

2.1. Cells, transfection and extraction of RNA and DNA

Human cervical HeLa cells and human 293T cells were grown in Dulbecco's modified Eagle's medium that contained 10% heat-inactivated fetal bovine serum, 50 units/ml penicillin, and 50 μg/ml streptomycin. The Jurkat line of human T-lymphoid cells was grown in similarly supplemented RPMI 1640 medium.

Transfections were performed by electroporation in a 4-mm-diameter cuvette using a Gene Pulser (Bio-Rad, Richmond, CA.) at 300 V and 975 μF for HeLa cells and at 260 V and 975 μF for Jurkat cells.

Genomic DNA was extracted from HeLa cells with a Wizard™ genomic DNA purification kit (Promega, Madison, WI.). Total RNA was extracted from HeLa cells and Jurkat cells using TRIzol™ reagent (Invitrogen, Carlsbad, CA.).

2.2. Construction of plasmids

The derivative of the expression vector pME18neo that encodes Flag-tagged wild-type Vpr, namely, pME18Neo-Fvpr, has been described previously [37,38]. To generate the control vector pME18Neo-Stop, in which a stop codon was inserted at the amino terminus of the *vpr* sequences, we performed PCR using pME18Neo-Fvpr as the template and primers VprSTOP (5′-ATCCGAATAAGCCCCAGAAGACC-3′) and PMER2 (5′-GGGGAGGTGTGGGAGGTTTT-3′). Then we subcloned the mutated *vpr* gene between the *Eco*RV and *Not*I sites of pME18Neo-Fvpr. To generate the expression vector for the *β-globin* gene, we amplified the *β-globin* gene, including three exons and two introns, by PCR with genomic DNA from HeLa cells as template and primers βG-1-EcoRV-5′ (5′-GGCGATATCCATGGTGCACCTGACTCCT-3′) and βG-end-XbaI-3′ (5′-GCTCTAGATTAGTGA-TACTTGTGGGC-3′). Then we cloned the amplified fragment between the *Eco*RV and *Xba*I sites of pBluescript II (SK$^+$) (Stratagene, La Jolla, CA.). The resulting construct was designated pSK-β-globin. The *Eco*RV and *Xba*I fragment of pSK-β-globin was excised and subcloned into pME18Neo-HA and encoded the following amino acid sequence: M-A-Y-P-Y-D-V-P-D-Y-A-COOH. To generate the expression vector for the *α-globin 2* gene, we amplified the *α-globin 2* gene, including three exons and two introns, by PCR with genomic DNA from HeLa cells as template and primers HBA2EcoRV (5′-ATCCATGGTGCTGTCTCCTGCC-3′) and HBANotI (5′-CAGCGGCCGCTTAACGGTATTTGGAGG-3′). Then we cloned the amplified fragment between the *Eco*RV and *Not*I sites of pME18Neo-HA.

Infectious molecular clone HIV-1 pNF462 was a kind gift from A. Adachi, Tokushima University, Japan [39]. To generate *env*-negative mutant designating pNF462Δ*env*, frame sift was introduced at *env* region of pNF462 as described below. Parental clone pNF462 was digested using *Bst*EII (TOYOBO, Osaka, Japan) and blunt-ended by KOD (TOYOBO). Then the fragment was self-ligated to introduce 5-base frame sift. To generate *vpr*-negative mutant designating pNF462Δ*env*Δ*vpr*, *Nde*I-*Sal*I fragment of pNL432Δ*vpr* were inserted at *Nde*I-*Sal*I site of pNF462Δ*env*. The generation of pNL432Δ*vpr* was described previously [40]. The expression plasmid of VSV-G, designated pCMV-G, has been previously described [41].

2.3. Reverse transcription-PCR

Samples of RNA were treated with RNase-free DNase I (Invitrogen) for 30 min at room temperature to remove genomic and plasmid DNA. Then 4 μg of total RNA were reverse-transcribed in the presence of oligo(dT) by SuperScript™ II Reverse Transcriptase (Invitrogen) in a total volume of 20 μl.

We amplified intron 1 of endogenous *α-globin 2* pre-mRNA by PCR using primers 5′HBA2E1N1 (5′-TTCTGGTCCCCACAGACTCA-3′) and 3′HBA2E3N1 (5′-

TTATTCAAAGACCAGGAAGGGC-3′) for the first PCR (15 cycles; see below for details of cycles), primers and 5′HBA2I1N2 (5′-GACCCACAGGCCACCCTCAA-3′) and 3′HBA2E3N2 (5′-GTGCTCACAGAAGCCAGGAACTTG-3′) for the second nested PCR or 5′HBA2E1N2 (5′-CCCACCATGGTGCTGTCTCC-3′) and 3′HBA2I2 (5′-CAGTGGCTTAGGAGCTGTGCAG-3′) for 35 cycles, as shown in Fig. 1D. We amplified endogenous *α-globin 2* mRNA by PCR (34 cycles) using primers 5′HBA2E1N1 (5′-TTCTGGTCCCCACAGACTCA-3′) and 3′HBA2E3N1 (5′-TTATTCAAAGACCAGGAAGGGC-3′). Introns 1 and 2 of unspliced *α-globin 2* pre-mRNA and spliced *α-globin 2* mRNA were detected by PCR with 0.5 μl of cDNA as template and the primers shown in Fig. 1D. To detect intron 1 of exogenous *α-globin 2* pre-mRNA, we performed PCR for 32 cycles with primers 5′HBA2I1 (5′-GACCCACAGGCCACCCTCAA-3′) and 3′HBA2E3 (5′-TAACGGTATTTGGAGGTCAGCACG-3′). To detect intron 2 of exogenous *α-globin 2* pre-mRNA, we performed PCR for 34 cycles with primers 5′HBA2E1 (5′-CGAGTATGGTGCGGAGGC-3′) and 3′HBA2I2. To detect exogenous *α-globin 2* mRNA, we performed PCR for 23 cycles with primers 5′HBA2E1 and 3′HBA2E3. We amplified *β-actin* mRNA by PCR (16 cycles) using primers 5′β-act (5′-CGTCGCCCTGGACTTCGAGCA-3′) and 3′β-act (5′-GCTGGAAGGTGGACAGCGAGGCCAGGA-3′). The details of each cycles of PCR were as follows: 2 min at 94 °C; then the indicated number of cycles of incubation at 94 °C for 30 s, at 60 °C for 30 s, and at 72 °C for 45 s; with a final 2-min extension at 72 °C. Reaction products were subjected to electrophoresis on a 2% agarose gel.

All products of PCR were cloned into pBluescript II (SK^+) and their identities were confirmed by nucleotide sequencing by the dideoxy chain-termination method with a CEQ™ 2000 DNA-analysis system (Beckman-Coulter, Fullerton, CA.).

2.4. Quantitative PCR

The real-time quantitative PCR of exogenous *α-globin 2* pre-mRNA was performed on LightCycler system (Roche Diagnostics, Mannheim, Germany) in the presence of LightCycler-FirstStart DNA Master SYBR Green I (Roche Diagnostics) using the following primers AG/1stF (5′-TTCTGGTCCCCACAGACTCA-3′) and AG/1stR (5′-TTATTCAAAGACCAGGAAGGGC-3′) for the first PCR, and AG/2nd/IN1F (5′-AGGCCACCCTCAACCGT-3′) and AGExon2R (5′-CTTGAAGTTGACCGGGTC-3′) for the second PCR. For normalization, quantitation of total *α-globin 2* RNA was performed using primers AG/1stF and AG/1stR for the first PCR, and AGExon2F (5′-GATGTTCCTGTCCTTCCC -3′) and AGExon2R for the second PCR. The first PCR product was treated with ExoSAP-IT™ (containing exonuclease I and shrimp alkaline phosphatase) to remove the first PCR primers according to the manufacturer's instructions (Amersham Bioscience, Uppsara, Sweden) and subjected to the second PCR.

2.5. RNase protection assay

RNase protection assays were performed with an RPA III kit (Ambion, Austin, TX.) according to the instructions in the manual from the manufacture. In brief, 10 μg of total RNA were allowed to hybridize with 8×10^4 cpm ^{32}P-labeled probe overnight at 46 °C. Unprotected single strand RNA was digested with RNases A and T1 and protected fragments were fractionated on a 5% polyacrylamide–7 M urea denaturing gel that was then exposed to an imaging plate (Fuji film, Tokyo, Japan).

For the generation of the probe for detection of splicing of *β-globin* pre-mRNA, we amplified full-length intron 1-exon 2 of *β-globin* by PCR using KOD plus DNA polymerase (TOYOBO) with genomic DNA from HeLa cells as template. We cloned the product of PCR into pBluescript II (SK^+) at the *Eco*RV site. The construct was verified by nucleotide sequencing. After linearization with *Not*I, an antisense probe was generated using a Riboprobe System (Promega) according to the manufacturer's standard protocol, 50 μCi [^{32}P]CTP (PerkinElmer, Boston, MA.) and T7 RNA polymerase. At the end of the reaction, 20 units of RNase-free DNase I (Promega) were added and incubation was continued at 37 °C for 15 min. The probe was then purified by gel filtration on a Sephadex G-50 spin column (Amersham Biosciences) to remove unincorporated nucleotides.

2.6. In vitro splicing assay

The pSK-β-globin plasmid including three exons and two introns, was linearized with *Bam*HI and then transcribed by the Riboprobe system (Promega) with T7 RNA polymerase and 50 μCi [^{32}P]CTP (PerkinElmer). Splicing reactions were carried out as described previously [42]. In brief, approximately 25 fmol of RNA transcript were incubated for 2 h at 30 °C with 60% (v/v) nuclear extract in Dignam's buffer D with 20 mM creatine phosphate, 3 mM $MgCl_2$, 0.8 mM ATP, and 2.6% (w/v) polyvinyl alcohol. HeLa nuclear extracts were prepared basically as described previously [43]. Transcripts were separated on a 7% polyacrylamide–7 M urea denaturing gel which was exposed to an imaging plate.

2.7. Western blotting

Cells were lyzed with a 1% solution of SDS 24 or 48 h after transfection. Lysates were suspended in Laemmli's [44] buffer and equal amounts of total protein were fractionated by SDS-PAGE (15% polyacrylamide). The separated proteins were transferred to a polyvinylidene difluoride membrane (Immobilon; Millipore, Bedford, MA.) for analysis by immunoblotting. Each membrane was blocked for 1 h in a 5% (w/v) solution of skim milk powder in PBS prior to incubation with anti-FLAG M2 monoclonal antibody (Sigma-Aldrich, St. Louis, MO.). Then the membrane was incubated with horseradish peroxidase-linked sheep antibodies against mouse IgG (Amersham Biosciences). Bands of immunoreac-

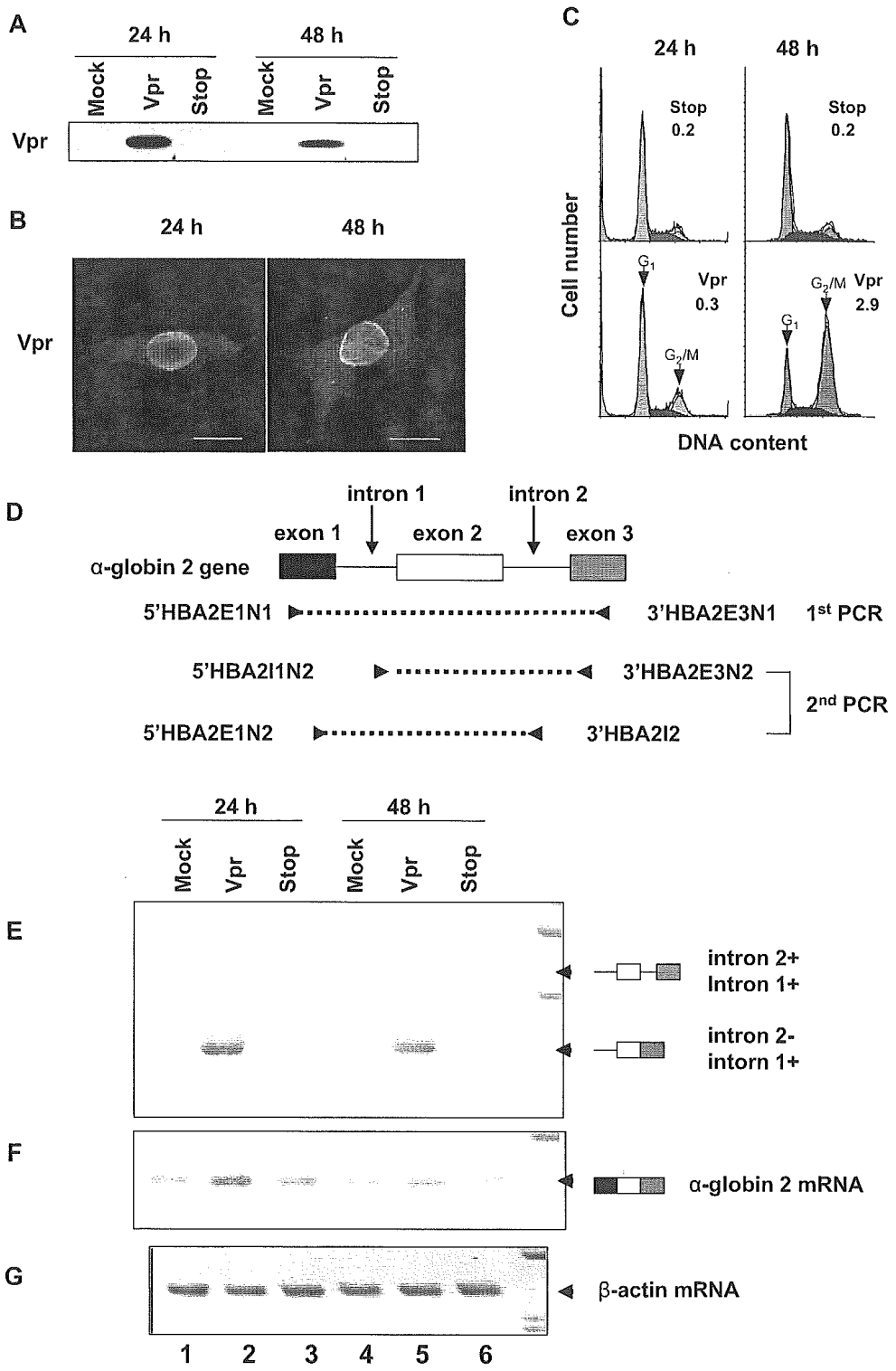

Fig. 1. Vpr prevented splicing of endogenous intron 1 of *α-globin 2* pre-mRNA in HeLa cells. HeLa cells were transfected with 30 μg of pME18Neo that encoded Flag-tagged wild-type Vpr (Vpr) or with 30 μg of control pME18Neo-Stop (Stop), or they were mock-transfected. Then, 24 and 48 h after transfection, cells were subjected to Western blotting (A), immunofluorescence (B), analysis of the cell cycle (C) and RT-PCR (D–G). (A) Western blotting of Vpr. Transfected cells were lyzed and then lysates containing 25 μg of protein were subjected to Western blotting analysis with the Flag-specific MAb M2. (B) Subcellular localization of Vpr. Transfected cells were subjected to immunofluorescence staining with Flag-specific MAb M2 and Alexa 488-conjugated goat antibodies against mouse IgG and analyzed by confocal laser scanning microscopy. Bar, 20 μm. (C) The DNA content of HeLa cells that expressed Vpr. Transfected cells were treated with the Flag-specific monoclonal antibody M2 and propidium iodide (PI). Cells that bound M2 were quantitated by flow cytometry. Arrowheads indicate peaks of cells at the G1 and G2/M phase. The ratio of cells at G2/M to those at G1 is indicated in the upper right of each graph. (D) Schematic representation of the human *α-globin 2* gene and the positions of primers used for nested RT-PCR. (E) Result of nested RT-PCR for examination of endogenous *α-globin 2* pre-mRNA. Total RNA was extracted from cells, as indicated, and subjected to the first RT-PCR with primers specific for exon 1 (5′HBA2E1N1) and

tive proteins were detected with the SuperSignal™ West Pico chemiluminescent substrate (Pierce, Rockford, IL.).

2.8. Immunofluorescence assay

HeLa cells, growing on coverslips, were examined 24 or 48 h after transfection by an immunofluoresence assay, as described previously [4].

2.9. Analysis of the cell cycle

HeLa cells were harvested 24 or 48 h after transfection and analyzed by flow cytometry for DNA content, as described previously [45].

2.10. Virus infection assay

To generate VSV-G pseudotyped virus, 293T cells (1×10^6 cells) were transfected with 5 μg of VSV-G expression vector together with 10 μg of pNF462Δ*env* or pNF462Δ*env*Δ*vpr*. Supernatants of transfected cells were harvested 24 h after transfection, filtered through 0.45-μm-pore-size filters and treated with DNase I (250 U, Sigma). The amount of HIV-1 p24 antigen was quantified with Lumipulse (Fujirebio, Tokyo Japan). HeLa cells were infected with VSV-G pseudotyped virus containing 100 ng of p24 antigen per 5×10^5 cells.

3. Results

3.1. Accumulation of the incompletely spliced form of endogenous α-globin 2 pre-mRNA

Vpr is involved in the import of the PIC of HIV-1 into the nuclei of non-dividing cells, in cellular differentiation, in the induction of cell cycle arrest at the G2/M phase, in immune suppression, and in enhancement of the replication of the HIV-1 itself [10–14,16,46]. However, although Vpr is a nucleophilic protein with non-classical nuclear localization signals [3,4], the function of Vpr in the nucleus remains to be clarified. To examine whether Vpr might affect splicing by the spliceosome, which is an important event in the nucleus, we transfected HeLa cells with pME18Neo-Fvpr that encoded Flag-tagged Vpr and with the control vector pME18Neo-Stop, in which a stop codon was located at the amino terminus of the *vpr* sequence. We extracted total cellular RNA and examined levels of unspliced endogenous human *α-globin 2* pre-mRNA and of spliced mRNA by nested RT-PCR (Fig. 1). We selected the human gene for *α-globin 2* as the cellular target gene, because it is a simple construct with only three exons and two introns and the length of the coding region, including two introns, is only 685 bps. Vpr was expressed at detectable levels within 24 h after transfection (Fig. 1A) and was localized predominantly in the nucleus and nuclear envelope (Fig. 1B). However, it was minimally effective in inducing G2 arrest (Fig. 1C). To our surprise *α-globin 2* pre-mRNA containing intron 1 but not intron 2 was clearly detectable in HeLa cells that had been transiently transfected with the Vpr-coding vector after the second PCR with forward primer 5′HBA2I1N2, which is located in intron 1, and reverse primer 3′HBA2E3N2, which is located in exon 3. We sequenced the fragment obtained by PCR and confirmed that the fragment was *α-globin 2* pre-mRNA that retained intron 1 but lacked intron 2 (data not shown). By contrast, pre-mRNA that contained intron 2 did not accumulate in cells that had been transfected with the Vpr-coding vector, or in cells transfected with the control vector pME18Neo-Stop and in mock-transfected cells. In addition, the second PCR with forward primer 5′HBA2E1N2, which spans exon 1, and reverse primer 3′HBA2I2, which spans intron 2, yielded neither of two possible types of pre-mRNA that contained intron 2 (data not shown). By contrast, in all cells transfected with the control vector pME18Neo-Stop and all mock-transfected cells, essentially all of the *α-globin 2* pre-mRNA had been spliced and spliced mRNA was produced (Figs. 1E, F). The levels of expression of *β-actin* mRNA were the same in all samples examined (Fig. 1G), as were levels of mRNAs that encoded GAPDH and L13a (data not shown). Our results indicated that splicing of *α-globin 2* pre-mRNA had been partially inhibited by overexpression of Vpr, allowing incompletely spliced pre-mRNA to accumulate. Moreover, we obtained similar results later in 48 h period after transfection, namely, during the time when Vpr is able to induced significant G2 arrest, as shown in Fig. 1C. These observations suggest that the Vpr-induced inhibition of splicing and G2 arrest are independent phenomena.

3.2. Vpr inhibits splicing of exogenous β-globin pre-mRNAs

To confirm that Vpr affects splicing of pre-mRNA in vivo, we selected the human gene for *β-globin*, which is also a comparatively simple construct. We produced a derivative of pME18Neo that included the *β-globin* gene, with three exons and two introns, under the control of the SRα promoter, as shown in Fig. 2A. Then, we transiently transfected HeLa cells with two pME18Neo expression vectors, namely, one that encoded Vpr and one that encoded *β-globin* pre-mRNA. We examined the splicing of *β-globin* pre-mRNA by RNase protection analysis using a ^{32}P-labeled antisense probe specific for *β-globin* pre-mRNA (Fig. 2). This probe was able to dif-

exon 3 (3′HBA2E3N1), and then the second nested RT-PCR with primers specific for intron 1 (5′HBA2I1N2) and exon 3 (3′HBA2E3N2), or with specific primers of exon 1 (5′HBA2E1N2) and intron 2 (3′HBA2I2). (F) Result of RT-PCR for examination of *α-globin 2* mRNA with primers specific for exon 1 (5′HBA2E1N1) and exon 3 (3′HBA2E3N1). (G) Result of RT-PCR for examination of *β-actin* mRNA. The products of PCR were subjected to electrophoresis on a 2% agarose gel. The data are representative of five independent experiments that gave similar results.

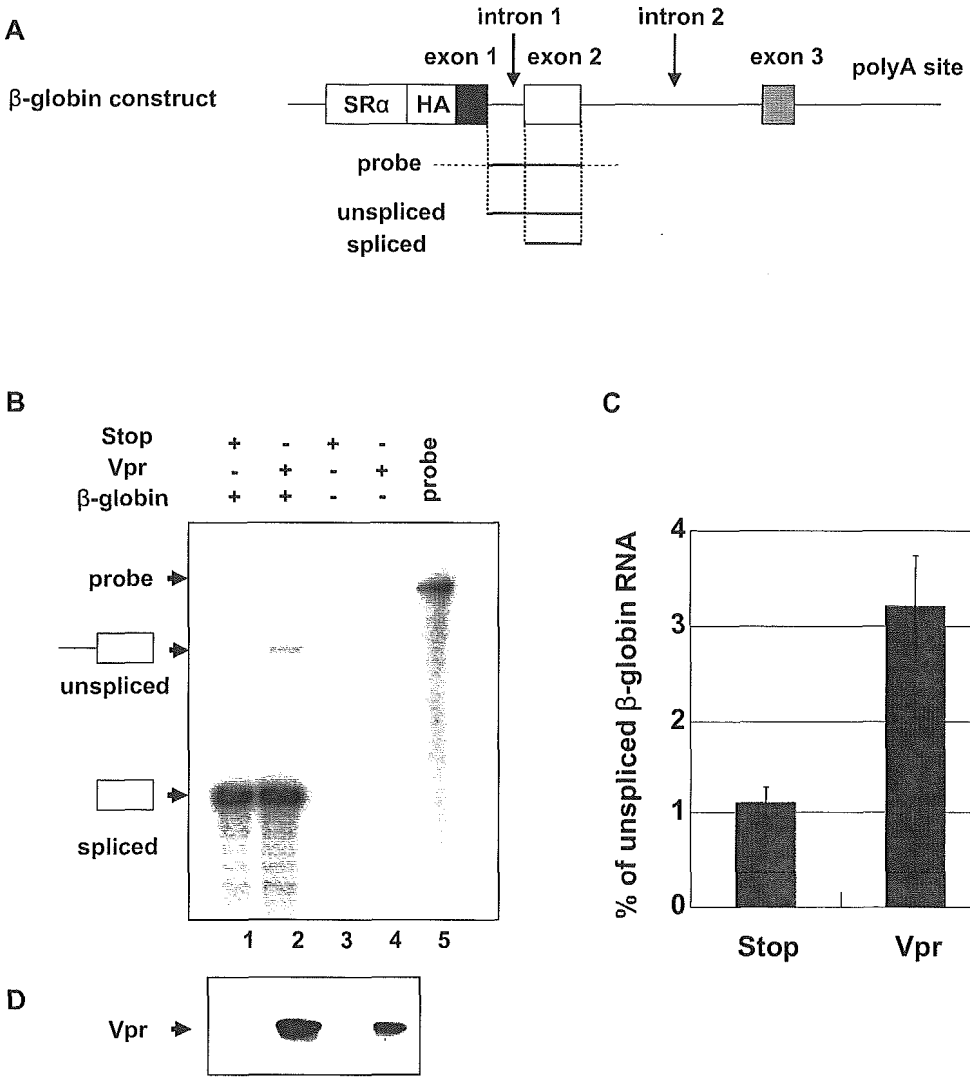

Fig. 2. Vpr inhibited the splicing of exogenous *β-globin* pre-mRNA in HeLa cells that had been transfected with a vector that encoded Vpr and a vector that encoded *β-globin* pre-mRNA. (A) The pME18Neo construct, showing the *β-globin* gene that contained three exons and two introns under the control of the SRα promoter. Bar shows the location of the antisense probe specific for *β-globin* pre-mRNA. In the RNase protection assay, this probe allowed discrimination between unspliced pre-mRNA and spliced mRNA, as indicated. B-D, HeLa cells were cotransfected with 25 μg of pME18Neo that encoded Flag-tagged wild-type Vpr (lanes 2 and 4) or control pME18Neo-Stop (lanes 1 and 3) together 5 μg of pME18Neo that encoded *β-globin* pre-mRNA (lanes 1 and 2). HeLa cells were harvested 24 h after transfection and divided into two portions. (B) Some cells were subjected to an RNase protection assay. Total RNA was extracted from cells and subjected to an RNase protection assay with the ^{32}P-labeled *β-globin* antisense probe. After treatment with RNases A and T1, the protected fragments were separated by electrophoresis on a 5% polyacrylamide–7 M urea denaturing gel. Arrows indicate positions of the intact probe, of unspliced *β-globin* RNA (intron 1+), and of spliced *β-globin* RNA (intron 1-). (C) Intensities of the unspliced and spliced β-globin pre-mRNA signals were quantitated using BAS2500 (Fujifilm Co., Tokyo, Japan) and percentage of the intensity of unspliced *β-globin* RNA against that of unspliced plus spliced *β-globin* RNA was calculated in each transfection. Each column and error bar represent the mean ± S.D. of results from three independent experiments. (D) The remaining cells were subjected to Western blotting with the Flag-specific monoclonal antibody M2 to determine levels of expression of Vpr. The data are representative of three independent experiments that gave similar results.

ferentiate unspliced *β-globin* pre-mRNA that contained intron 1 from spliced mRNA, as shown in Fig. 2A. Protected fragments were fractionated on a 5% acrylamide–7 M urea denaturing gel. We found that, 24 h after transfection, pre-mRNA that contained intron 1 modestly accumulated in cells that had been transfected with pME18Neo-Fvpr plus the *β-globin* expression vector, as compared to levels in HeLa cells that had been transfected with pME18Neo-Stop plus the *β-globin* expression vector (Fig. 2B, lanes 1 and 2). The percentage of unspliced *β-globin* RNA against total *β-globin* RNA in HeLa cells that had been transfected with pME18Neo-Fvpr was approximately threefold higher than that in HeLa cells that had been transfected with control vector pME18Neo-Stop (Fig. 2C). Thus, it appeared that Vpr had modestly inhibited splicing of exogenous *β-globin* pre-mRNA in vivo. Furthermore, *β-globin* pre-mRNA was spliced and spliced *β-globin* mRNA also accumulated. By contrast, no bands of unspliced pre-mRNA and spliced mRNA were detected in the analysis of RNA from HeLa cells had not been transfected with the *β-globin* expression vector (Fig. 2B, lanes 3 and 4), indicating the absence of endogenous *β-globin* pre-mRNA and spliced mRNA in this system. Moreover, we obtained similar

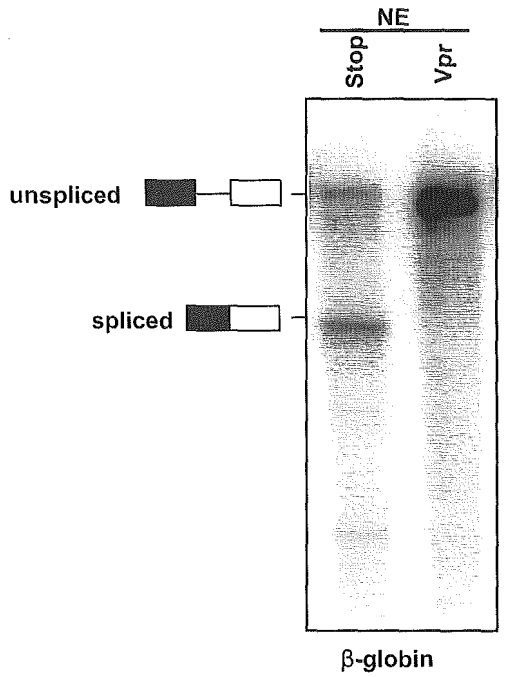

Fig. 3. Vpr inhibited splicing in vitro. HeLa cells were transfected with 30 μg of pME18Neo that encoded Flag-tagged wild-type Vpr (Vpr) or 30 μg of control pME18Neo-Stop (Stop). Then, 24 h after transfection, nuclear extracts (NE) were prepared from cells and subjected to in vitro splicing assay with ^{32}P-labeled *β-globin* pre-mRNA as substrate. The products were separated on a 7% polyacrylamide–7 M urea denaturing gel.

results in RNase protection analysis with a derivative of pME18Neo that included the *α-globin 2* gene with three exons and two introns under the control of the SRα promoter (data not shown). Since our findings tended to confirm the results of amplification by nested RT-PCR of the endogenous pre-mRNA, it appeared that Vpr might partially inhibit the splicing of *β-globin* and *α-globin 2* pre-mRNAs in vivo.

3.3. Vpr inhibits pre-mRNA splicing in vitro

To obtain definitive evidence that Vpr acts on splicing, we included this protein in in vitro splicing assays with a nuclear extract (NE) of HeLa cells that had been transiently transfected with either pME18Neo-Fvpr or pME18Neo-Stop (Fig. 3). As a substrate we used ^{32}P-labeled *β-globin* pre-mRNA with a G capped at the 5′ end. As expected, the splicing of *β-globin* was dramatically suppressed by the nuclear extract from HeLa cells that expressed Vpr. By contrast, splicing activity of a nuclear extract from HeLa cells that had been transfected with pME18Neo-Stop was sufficient to splice *β-globin* pre-mRNA. This in vitro splicing assay demonstrated that Vpr regulated the splicing of *β-globin* pre-mRNA.

3.4. Vpr inhibits splicing of exogenous α-globin 2 pre-mRNA

As shown in Fig. 1, amplification of endogenous *α-globin 2* pre-mRNA by nested RT-PCR demonstrated that pre-mRNA that contained only intron 1 and not intron 2 accumulated in the presence of Vpr. Thus, inhibition of splicing upon expression of Vpr might be sequence-specific. Therefore, we examined the effects of the expression of Vpr on cellular splicing by RT-PCR using total RNA from Jurkat cells that had been transfected with pME18Neo-Fvpr or pME18Neo-Stop and a derivative of pME18Neo that included the *α-globin 2* gene (Fig. 4). In this experiment, we used Jurkat cells, a line of human T-lymphoid cells that is permissive with respect to infection by HIV-1 and from which it is not possible to amplify the endogenous *α-globin 2* pre-mRNA by nested RT-PCR. In our analysis, 24 h after transfection, we detected three products amplification by RT-PCR of pre-mRNA. They contained intron 1 but not intron 2 (Fig. 4Bb), intron1 and intron 2 (Fig. 4Ba, Bc), and intron 2 but not intron 1 (Fig. 4Bd) both in the absence and in the presence of Vpr. The levels of *β-actin* mRNA were similar in all samples examined (Fig. 4B). These results indicate that splicing of intron 1 might be partially inhibited by Vpr, while splicing of intron 2 was unaffected. We obtained similar results in HeLa cells (data not shown). Collectively, our results indicate that Vpr of HIV-1 is involved in selective inhibition during the splicing of cellular pre-mRNAs.

3.5. Vpr expressed from an HIV-1 provirus accumulates endogenous α-globin 2 pre-mRNA

To monitor the potential of Vpr to inhibit the splicing of cellular pre-mRNAs, we assessed whether HIV-1 infection accumulated endogenous *α-globin 2* pre-mRNA. HeLa cells were infected with 100 ng equivalent of p24 of VSV-G pseudotyped HIV-1 *vpr*$^+$ or *vpr*$^-$ virus. Then 24 h after infection, total RNA was isolated from HeLa cells and real-time quantitative RT-PCR were carried out to quantitate the level of endogenous *α-globin 2* pre-mRNA. The level of total *α-globin 2* RNA was measured for normalization and fold-production of the level of *α-globin 2* pre-mRNA that contains intron 1 was quantified (Fig. 5B). Interestingly, a higher level of *α-globin 2* pre-mRNA that contains intron 1 was detected in HeLa cells infected with *vpr*$^+$ virus than that in HeLa cells infected with *vpr*$^-$ virus. This result indicated that Vpr produced from an HIV-1 provirus was sufficient to accumulate endogenous *α-globin 2* pre-mRNA in an infection system as well as in a transient transfection system.

4. Discussion

Our present results lead to three major conclusions. First, the present study reveals that Vpr, when expressed transiently in cells, can regulate the splicing reaction of cellular pre-mRNA both in vivo and in vitro. Using RT-PCR and RNase protection assays, we showed that Vpr induced the accumulation of unspliced forms of *α-globin 2* and *β-globin* pre-mRNAs in HeLa cells that expressed Vpr. We confirmed the modulation of splicing by Vpr in in vitro splicing assays

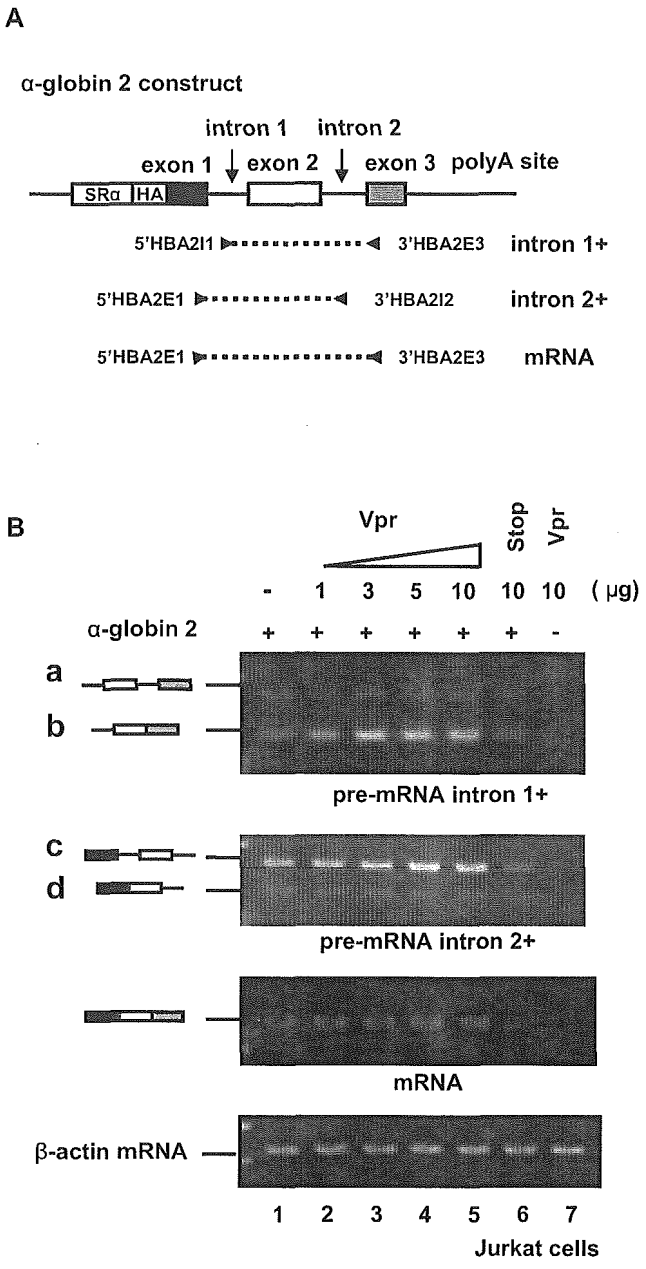

Fig. 4. Analysis by RT-PCR of exogenous *α-globin 2* pre-mRNA in Jurkat cells that had been transfected with a vector that encoded Vpr and a vector that encoded *α-globin 2* pre-mRNA. (A) The pME18Neo construct including *α-globin 2* gene that contained three exons and two introns under the control of the SRα promoter and the position of each primer used for RT-PCR. (B) Jurkat cells were transfected with 1, 3, 5 and 10 μg of pME18Neo that encoded Flag-tagged wild-type Vpr (lanes 2–5), 10 μg of control pME18Neo-Stop (lane 6) or none of this plasmid (lane 1), and 1 μg of pME18Neo that encoded *α-globin 2* pre-mRNA (lanes 1 and 2). Then, 24 h after transfection, RT-PCR was performed with a pair of primers specific for *α-globin 2* pre-mRNA, and products of PCR were subjected to electrophoresis on a 2% agarose gel. RT-PCR to amplify cellular *β-actin* mRNA was performed as a control. Total amounts of DNA were equalized by addition of control pME18neo. The data are representative of results of three independent experiments.

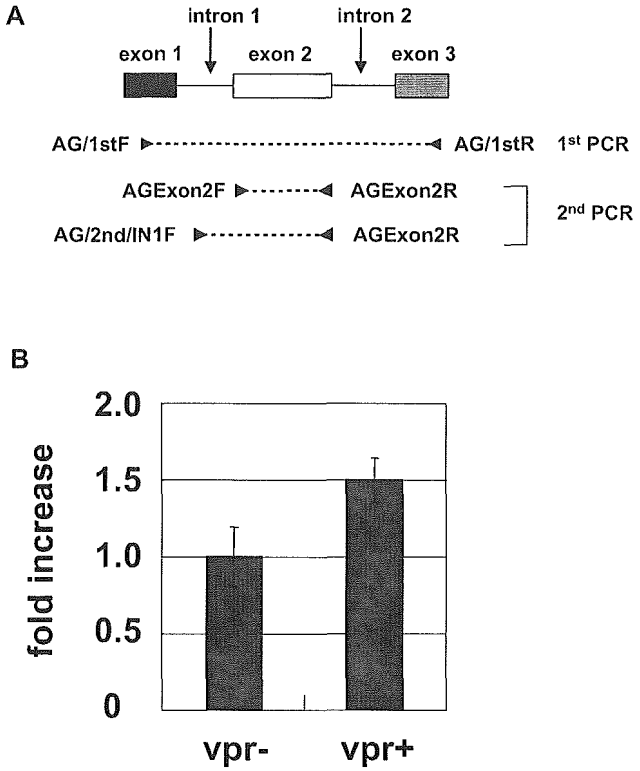

Fig. 5. Vpr expressed from an HIV-1 provirus accumulates endogenous α-globin2 pre-mRNA. Vesicular stomatitis virus G protein (VSV-G) pseudotyped HIV-1 viruses were harvested from 293T cell cultures 24 h after cotransfection with VSV-G expression vector together with pNF462Δ*env* or pNF462Δ*env*Δ*vpr*. HeLa cells (5×10^5) were infected with 100 ng of p24 antigen equivalent of pseudotyped viruses. Two hours after infection, cells were washed with serum-free medium twice and cultured with fresh medium containing 10% fetal bovine serum. Then, 24 h after infection, quantitative RT-PCR was performed using specific primers for total *α-globin 2* RNA or *α-globin 2* pre-mRNA that contains intron 1. (A) Schematic representation of *α-globin 2* gene and the position of primers used for quantitative RT-PCR. (B) Fold increase of the level of *α-globin 2* pre-mRNA that contains intron 1. Signals of amplification products were normalized by those of total *α-globin 2* RNA. Each column and error bar represent the mean ± S.D. of results from three independent experiments.

as follows. The splicing of *β-globin* pre-mRNA was dramatically suppressed when a nuclear extract from HeLa cells that expressed Vpr was added to an in vitro splicing system, suggesting that Vpr had an effect on the splicing machinery. The level of inhibition of splicing by Vpr was modest in vivo but high in vitro. The reason why such difference arose between in vivo and in vitro was not clear, but there was a possibility that some factors that could alleviate the inhibition of splicing by Vpr in vivo existed at low levels or lacked in HeLa nuclear extract that used in the in vitro splicing assay. Thus, the mechanism by which Vpr inhibits pre-mRNA splicing appears to be novel. Second, although the inhibition of splicing induced by Vpr was not as strong as that shown in a transient transfection system, we also indicated strong evidence that Vpr expressed from an HIV-1 provirus was sufficient to accumulate endogenous α-globin 2 pre-mRNA in an infection system using VSV-G pseudotyped HIV-1 vpr^+ or vpr^- virus. Third, our results also indicate the potential sequence-specific nature of the Vpr-induced modulation of splicing. Amplification of endogenous *α-globin 2* pre-mRNA by nested RT-PCR demonstrated that pre-mRNA that contained only intron 1 and not intron 2 accumulated in presence of Vpr.

Moreover, RT-PCR with total RNA from Jurkat cells that had been transfected with a pME18Neo-Fvpr plus a derivative of a pME18Neo that included the *α-globin 2* gene revealed that Vpr-induced an increase in the accumulation of all products of pre-mRNA that contained intron 1. Further studies are required to clarify why Vpr inhibit splicing of the particular intron.

The NS1 protein of influenza virus [26,27,47] and the ICP27 protein of HSV [29–31,48] have been reported to inhibit the splicing of cellular pre-mRNA, perhaps as a part of the mechanism for shutting down the synthesis of host proteins. The NS1 protein binds to U6 small nuclear RNA, inhibiting the formation of U4/U6 and U2/U6 complex [47], while ICP27 inhibits splicing by interfering with assembly of spliceosomes [31]. In addition, it has been proposed that ICP27 interacts with SRPK1 and inhibits splicing by altering the phosphorylation of SR protein [48]. Moreover, ICP27 also interacts with spliceosome-associated protein 145 and inhibits its splicing prior to the first catalytic step [30]. It has been demonstrated that Vpr binds to ribonucleic acid via a process that requires the carboxy-terminal basic domain of the protein (in particular the helical 70–80 domain) [49], which suggests the possibility of a functional association with pre-mRNA. Indeed, we have preliminary evidence (Kuramitsu and Aida, personal communication) that a carboxy-terminal domain of Vpr is essential for the inhibition of splicing. Therefore, our present results and the previous demonstration that NS1 and ICP27 can associate with spliceosomes that contained splicing intermediates suggest that Vpr might interact with spliceosomes, which inhibit splicing at the stage when the splicing complex is formed. It is also possible that Vpr inhibits splicing by preventing pre-mRNA from association with spliceosomes or stabilizing pre-mRNA through the association with pre-mRNA. These issues will be further elucidated.

The correlations between the novel ability of Vpr to inhibit splicing of cellular pre-mRNA and the previously characterized functions of Vpr in phenomena such as LTR activation [16], apoptosis [50] and G2 arrest [10–13], suggest some intriguing possibilities. Splicing and transcription are tightly coupled [51]. For example, spliceosomal UsnRNP forms a complex with elongation factor TAT-SF1, which associates with RNA polymerase II (pol II) via the carboxy-terminal domain (CTD) kinase PTEFb. This UsnRNP-TAT-SF1 complex stimulates both transcription and splicing in vitro [52]. Kino and Pavlakis [53] have reported that hsRBP7, a subunit of pol II, bind Vpr in a yeast two-hybrid screening assay. This observation strongly suggests that Vpr might regulate transcription via an interaction with hsRBP7 and might then coincidentally, participate in the splicing reaction. Moreover, apoptosis and splicing influence one another. For example, the cellular apoptosis-promoting factor TIA-1 is a regulator of the splicing of pre-mRNA [54,55]. However, it remains unclear whether Vpr can inhibit splicing via these two processes. By contrast, Vpr-induced G2 arrest might be a key event related to the inhibition of splicing by Vpr. Roshal et al. [56] showed that treatment with LY294002, an inhibitor of phosphatidylinositol 3-kinase, alleviated Vpr-induced G2 arrest in HeLa cells. Moreover, recent reports indicated that RNA processing is also the target of several signal-transduction pathways, including phosphatidylinositol 3-kinase pathway [57,58]. However, in the present study, we detected the accumulation of pre-mRNA during the 24-h period after transfection, namely, during the time when Vpr is unable to induce G2 arrest. This result clearly indicates that the inhibition of splicing by Vpr is not the result of G2 arrest. Further studies are required to determine whether inhibition of the splicing of pre-mRNA influences the induction of G2 arrest by Vpr.

The generation of the 2 or 4-kb form of HIV-1 RNA from unspliced 9-kb genomic RNA by splicing is orchestrated by *cis* elements like exonic splicing enhancers (ESEs), exonic splicing silencers (ESSs), intronic splicing silencers, and the viral protein Rev [59–64]. It has been suggested that, Rev-mediated nuclear export of incompletely spliced HIV-1 RNA regulates splicing of HIV-1 RNA [63]. However, splicing of HIV-1 RNA is also controlled by many cellular splicing factors, such as SR proteins and heterogeneous nuclear ribonucleoproteins (hnRNPs). For example, the generation of tat mRNA is regulated via splicing acceptor site A3. Splicing at the A3 site is regulated by ESS2p [62], ESE2 [60] and ESS2 [61]. The ribonucleoprotein designated hnRNP H binds to the ESS2p element to repress activity at splice site A3. SC35 binds to the ESE2 to activate splicing, whereas hnRNP A1 binds ESS2 to repress splicing. ESE2 and ESS2 overlap and binding of hnRNP A1 to ESS2 masks binding site for SC35 and inhibits splicing at the A3 site. By contrast, it has been suggested that Vpr acts multifunctionally via interactions with numerous cellular partner molecules, such as the 14-3-3, the p300/CREB-binding protein, and the importin α [53]. Therefore, it is possible that Vpr might be associated not only with host splicing but also with the alternative splicing of HIV-1 RNA. However, we do not know whether Vpr interacts with regulators of splicing that control splicing of HIV-1 RNA. Thus, while our present results suggest that Vpr inhibits splicing of cellular pre-mRNA, it remains to be determined whether Vpr regulates splicing of the HIV-1 genome. Our understanding of the life cycle of HIV-1 and the progression of AIDS pathogenesis will be enhanced as we improve our understanding of the roles of Vpr both in cellular splicing and in the life cycle of HIV-1.

Acknowledgments

This work was supported in part by a grant for AIDS Research from the Japan Health Sciences Foundation (KA21502); by a Health Sciences Research Grant from the Ministry of Hearth, Labour and Welfare of Japan (Research on HIV/AIDS 13110201 and 16150301), by a grant-in-aid for Scientific Research on Priority Areas from the Ministry of Education, Culture, Sports, Science, and Technology

(MEXT) of Japan (1402113, 15019115, and 16017304) and by a President's Special Research Grant from RIKEN.

We thank Dr. K. Nagata, Mrs. K. Sugiyama and K. Murano (University of Tsukuba, Ibaraki, Japan) for helpful discussions and technical advice and to Mrs. K. Muneta and Mrs. K. Kimata (Retrovirus Research Unit, RIKEN) for their skilled technical assistance.

References

[1] X. Yuan, Z. Matsuda, M. Matsuda, M. Essex, T.H. Lee, Human immunodeficiency virus vpr gene encodes a virion-associated protein, AIDS Res. Hum. Retroviruses 6 (1990) 1265–1271.

[2] E.A. Cohen, G. Dehni, J.G. Sodroski, W.A. Haseltine, Human immunodeficiency virus vpr product is a virion-associated regulatory protein, J. Virol. 64 (1990) 3097–3099.

[3] Y. Jenkins, M. McEntee, K. Weis, W.C. Greene, Characterization of HIV-1 vpr nuclear import: analysis of signals and pathways, J. Cell Biol. 143 (1998) 875–885.

[4] M. Kamata, Y. Aida, Two putative alpha-helical domains of human immunodeficiency virus type 1 Vpr mediate nuclear localization by at least two mechanisms, J. Virol. 74 (2000) 7179–7186.

[5] N.K. Heinzinger, M.I. Bukinsky, S.A. Haggerty, A.M. Ragland, V. Kewalramani, M.A. Lee, H.E. Gendelman, L. Ratner, M. Stevenson, M. Emerman, The Vpr protein of human immunodeficiency virus type 1 influences nuclear localization of viral nucleic acids in nondividing host cells, Proc. Natl. Acad. Sci. USA 91 (1994) 7311–7315.

[6] R.I. Connor, B.K. Chen, S. Choe, N.R. Landau, Vpr is required for efficient replication of human immunodeficiency virus type-1 in mononuclear phagocytes, Virology 206 (1995) 935–944.

[7] P. Gallay, V. Stitt, C. Mundy, M. Oettinger, D. Trono, Role of the karyopherin pathway in human immunodeficiency virus type 1 nuclear import, J. Virol. 70 (1996) 1027–1032.

[8] R.A. Fouchier, B.E. Meyer, J.H. Simon, U. Fischer, A.V. Albright, F. Gonzalez-Scarano, M.H. Malim, Interaction of the human immunodeficiency virus type 1 Vpr protein with the nuclear pore complex, J. Virol. 72 (1998) 6004–6013.

[9] S. Popov, M. Rexach, L. Ratner, G. Blobel, M. Bukrinsky, Viral protein R regulates docking of the HIV-1 preintegration complex to the nuclear pore complex, J. Biol. Chem. 273 (1998) 13347–13352.

[10] J. He, S. Choe, R. Walker, P. Di Marzio, D.O. Morgan, N.R. Landau, Human immunodeficiency virus type 1 viral protein R (Vpr) arrests cells in the G2 phase of the cell cycle by inhibiting p34cdc2 activity, J. Virol. 69 (1995) 6705–6711.

[11] J.B. Jowett, V. Planelles, B. Poon, N.P. Shah, M.L. Chen, I.S. Chen, The human immunodeficiency virus type 1 vpr gene arrests infected T cells in the G2 + M phase of the cell cycle, J. Virol. 69 (1995) 6304–6313.

[12] F. Re, D. Braaten, E.K. Franke, J. Luban, Human immunodeficiency virus type 1 Vpr arrests the cell cycle in G2 by inhibiting the activation of p34cdc2-cyclin B, J. Virol. 69 (1995) 6859–6864.

[13] M.E. Rogel, L.I. Wu, M. Emerman, The human immunodeficiency virus type 1 vpr gene prevents cell proliferation during chronic infection, J. Virol. 69 (1995) 882–888.

[14] B. Poon, K. Grovit-Ferbas, S.A. Stewart, I.S. Chen, Cell cycle arrest by Vpr in HIV-1 virions and insensitivity to antiretroviral agents, Science 281 (1998) 266–269.

[15] M. Hrimech, X.J. Yao, F. Bachand, N. Rougeau, E.A. Cohen, Human immunodeficiency virus type 1 (HIV-1) Vpr functions as an immediate-early protein during HIV-1 infection, J. Virol. 73 (1999) 4101–4109.

[16] W.C. Goh, M.E. Rogel, C.M. Kinsey, S.F. Michael, P.N. Fultz, M.A. Nowak, B.H. Hahn, M. Emerman, HIV-1 Vpr increases viral expression by manipulation of the cell cycle: a mechanism for selection of Vpr in vivo, Nat. Med. 4 (1998) 65–71.

[17] V. Ayyavoo, A. Mahboubi, S. Mahalingam, R. Ramalingam, S. Kudchodkar, W.V. Williams, B.H. Hahn, M. Emerman, HIV-1 Vpr suppresses immune activation and apoptosis through regulation of nuclear factor kappa B, Nat. Med. 3 (1997) 1117–1123.

[18] M. Nishizawa, M. Kamata, T. Mojin, Y. Nakai, Y. Aida, Induction of apoptosis by the Vpr protein of human immunodeficiency virus type 1 occurs independently of G(2) arrest of the cell cycle, Virology 276 (2000) 16–26.

[19] E. Jacotot, L. Ravagnan, M. Loeffler, K.F. Ferri, H.L. Vieira, N. Zamzami, P. Costantini, S. Druillennec, J. Hoebeke, J.P. Briand, T. Irinopoulou, E. Daugas, S.A. Susin, D. Cointe, Z.H. Xie, J.C. Reed, B.P. Roques, G. Kroemer, The HIV-1 viral protein R induces apoptosis via a direct effect on the mitochondrial permeability transition pore, J. Exp. Med. 191 (2000) 33–46.

[20] S.A. Stewart, B. Poon, J.Y. Song, I.S. Chen, Human immunodeficiency virus type 1 vpr induces apoptosis through caspase activation, J. Virol. 74 (2000) 3105–3111.

[21] K. Muthumani, D.S. Hwang, B.M. Desai, D. Zhang, N. Dayes, D.R. Green, D.B. Weiner, HIV-1 Vpr induces apoptosis through caspase 9 in T cells and peripheral blood mononuclear cells, J. Biol. Chem. 277 (2002) 37820–37831.

[22] T. Roumier, H.L. Vieira, M. Castedo, K.F. Ferri, P. Boya, K. Andreau, S. Druillennec, N. Joza, J.M. Penninger, B. Roques, G. Kroemer, The C-terminal moiety of HIV-1 Vpr induces cell death via a caspase-independent mitochondrial pathway, Cell Death Differ. 9 (2002) 1212–1219.

[23] C.M. de Noronha, M.P. Sherman, H.W. Lin, M.V. Cavrois, R.D. Moir, R.D. Goldman, W.C. Greene, Dynamic disruptions in nuclear envelope architecture and integrity induced by HIV-1 Vpr, Science 294 (2001) 1105–1108.

[24] J.F. Caceres, A.R. Kornblihtt, Alternative splicing: multiple control mechanisms and involvement in human disease, Trends Genet. 18 (2002) 186–193.

[25] A.I. Lamond, D.L. Spector, Nuclear speckles: a model for nuclear organelles, Nat. Rev. Mol. Cell Biol. 4 (2003) 605–612.

[26] Y. Lu, X.Y. Qian, R.M. Krug, The influenza virus NS1 protein: a novel inhibitor of pre-mRNA splicing, Genes Dev. 8 (1994) 1817–1828.

[27] P. Fortes, A. Beloso, J. Ortin, Influenza virus NS1 protein inhibits pre-mRNA splicing and blocks mRNA nucleocytoplasmic transport, EMBO J. 13 (1994) 704–712.

[28] M.A. Hardwicke, R.M. Sandri-Goldin, The herpes simplex virus regulatory protein ICP27 contributes to the decrease in cellular mRNA levels during infection, J. Virol. 68 (1994) 4797–4810.

[29] W.R. Hardy, R.M. Sandri-Goldin, Herpes simplex virus inhibits host cell splicing, and regulatory protein ICP27 is required for this effect, J. Virol. 68 (1994) 7790–7799.

[30] H.E. Bryant, S.E. Wadd, A.I. Lamond, S.J. Silverstein, J.B. Clements, Herpes simplex virus IE63 (ICP27) protein interacts with spliceosome-associated protein 145 and inhibits splicing prior to the first catalytic step, J. Virol. 75 (2001) 4376–4385.

[31] A. Lindberg, J.P. Kreivi, Splicing inhibition at the level of spliceosome assembly in the presence of herpes simplex virus protein ICP27, Virology 294 (2002) 189–198.

[32] M.H. Malim, J. Hauber, S.Y. Le, J.V. Maizel, B.R. Cullen, The HIV-1 rev trans-activator acts through a structured target sequence to activate nuclear export of unspliced viral mRNA, Nature 338 (1989) 254–257.

[33] U. Fischer, J. Huber, W.C. Boelens, I.W. Mattaj, R. Luhrmann, The HIV-1 Rev activation domain is a nuclear export signal that accesses an export pathway used by specific cellular RNAs, Cell 82 (1995) 475–483.

[34] M. Fornerod, M. Ohno, M. Yoshida, I.W. Mattaj, CRM1 is an export receptor for leucine-rich nuclear export signals, Cell 90 (1997) 1051–1060.

[35] M. Neville, F. Stutz, L. Lee, L.I. Davis, M. Rosbash, The importin-beta family member Crm1p bridges the interaction between Rev and the nuclear pore complex during nuclear export, Curr. Biol. 7 (1997) 767–775.